Biointerface Research in Applied Chemistry
Open-Access Journal (ISSN: 2069-5837)

Article
Volume 16, Issue 4, 2026, 104
https://doi.org/10.33263/BRIAC164.104

Coupling of Some Fluoride Derivatives to VEGFR-1 and EPHB4 Using a Theoretical Model

Bonilla-Zavaleta Enrique [1], Rosas-Nexticapa Marcela [1,*], Alvarez-Ramirez Magdalena [1], Melgarejo-Gutiérrez Montserrat Alheli [2], Rascon-Diaz Martha Paola [3], Ramírez-Higuera Abril [4]

[1] Nutrition Laboratory, Faculty of Nutrition, University of Veracruz, Medicos y s/n Odontologos 910210, Unidad del Bosque, Xalapa, Mexico
[2] Faculty of Medicine, University of Veracruz, Médicos y Odontologos s/n C.P. 91010, Unidad del Bosque, Xalapa, Mexico
[3] Food Research and Development Center. University of Veracruz. Av. Castelazo Ayala Sn, Industrial Ánimas, 91190 Xalapa-Enríquez, Veracruz, Mexico
[4] Institute of Basic Sciences. University of Veracruz. Av. Castelazo Ayala Sn, Industrial Ánimas, 91192 Xalapa-Enríquez, Veracruz, Mexico.
* Correspondence: rosasnm@uv.mx;

Received: 28.04.2026; Accepted: 28.05.2026; Published: 15.08.2026

Abstract: Several drugs such as sanguinarine, NVP-VHG712, QDAU5, and VDAU1-11 have been used to treat some cancer cells; however, their interaction with VEGFR-1 AND EPHB4 is not clear. For this reason, in this study, the coupling of some fluoride derivatives (1-36) with VEGFR-1 AND EPHB4 was determined using the 2VWX and 3HNG proteins as theoretical tools. In addition, sanguinarine, NVP-BHG712, QDAU5, and VDAU-11 were used as controls in the DockingServer program. The results showed differences in the number of amino acid residues involved in the coupling of fluoride analogs with the 2VWX and 3HNG proteins compared with the controls. Besides, the fluoride derivatives 6 and 10 have a higher affinity for the 2VWXprotein surface compared to the compounds 1, 3-5, 7-9, and 11-36. Other data indicate that fluorinated analogs 6, 12, 27, and 29 have a higher affinity for the 3HNG protein compared to the compounds 1-5, 7-11, 13-26, and 30-36. In conclusion, these data suggest that the fluorinated derivatives 6, 10, 12, 27, and 29 could act as inhibitors of EGFR-1 and EPHB4. Therefore, these compounds could be good candidates for evaluating their activity in some biological model.

Keywords: Cancer; VEGFR-1; EPHB4; fluoride.

1. Introduction

Angiogenesis is a physiological process by which new blood vessels are formed from pre-existing vessels [1-3]. This phenomenon is conditioned by the activation and/or release of several biomolecules, including ephrin type-B receptor 4 (EphB4) [4, 5], interleukins [6-8], tumor necrosis factor-alpha [9], vascular endothelial growth factor (VEGF) [10-12], epidermal growth factor [13], and others. It is important to mention that a study indicates that EphB4 may be involved in the promotion, proliferation, invasion, and angiogenesis of human colorectal cancer [14]. Other data indicate that EphB4 exerts pro-tumoral and anti-tumoral roles of EphA4 on T regulatory cells and tumor-associated macrophages during HNSCC tumor progression [15]. Other studies have shown that EphB4 overexpression is associated with advanced stages of ovarian, head and neck, and breast cancer [16, 17]. Furthermore, a report indicates that

EphB4 is implicated in the development of colorectal and prostate cancer, which can result in a reduced quality of life for patients [18, 19].

On the other hand, some studies suggest that the EphrinB2/EphB4 signaling pathway plays a crucial role in VEGF-mediated angiogenesis [20]. Furthermore, a report indicates that EphrinB2 expression is induced by a stress response in murine embryonic stem cells via the VEGF-Notch signaling pathway. [21]. It is important to note that the VEGF-Notch pathway is a mechanism that regulates the formation of new blood vessels (angiogenesis). [22]. In addition, some studies indicate that VEGF may mediate angiogenesis in cancer [23]. In this way, some data showed that overexpression of VEGF and its receptors (VEGF-R1, VEGF-R2, and VEGF-R3) may be overexpressed in some cancer cells [24-26]; for example, a study indicates that the vascular endothelial growth factor C/vascular endothelial growth factor receptor-3 (VEGFR-3) axis plays an important role in tumor lymphangiogenesis [27]. Other data suggest that both VEGFR-1 and VEGFR-2 could be expressed in malignant melanocytes [28]. Finally, a study showed that VEGFR-2 and VEGFR-3 are overexpressed in ovarian cancer patients [29]. All this data indicates that the overexpression of EphB4, VEGF, and their receptors may be associated with the growth of cancer cells; this phenomenon is supported by a study showing that the NVP-BHG712 drug (an EphB4 antagonist) inhibits VEGF-induced angiogenesis [30]. Besides, a study showed that compound VDAU-11 (N-(5-(4-(3-(3-chlorophenyl)ureido)phenyl)pyridin2-yl)acrylamide) acts as a triple inhibitor of VEGFR2/TIE-2/EphB4 using an in vitro model [31]. All these data indicate that some drugs can modulate the biological activity of EphB4 and VEGF; however, the interaction between them remains unclear, possibly due to their different chemical structures. Based on this hypothesis, the objective of this study was to determine the coupling of some fluorinated derivatives to EphB4 and VEGF-R1 using the 2VWX and 3HNG proteins as theoretical tools in the DockingServer program.

2. Materials and Methods

2.1. Chemical structure.

Fluoride derivatives (Figures 1 and 2; Table 1) were used to determine their interaction with the VEGFR-1 AND EPHB4 surfaces as follows:

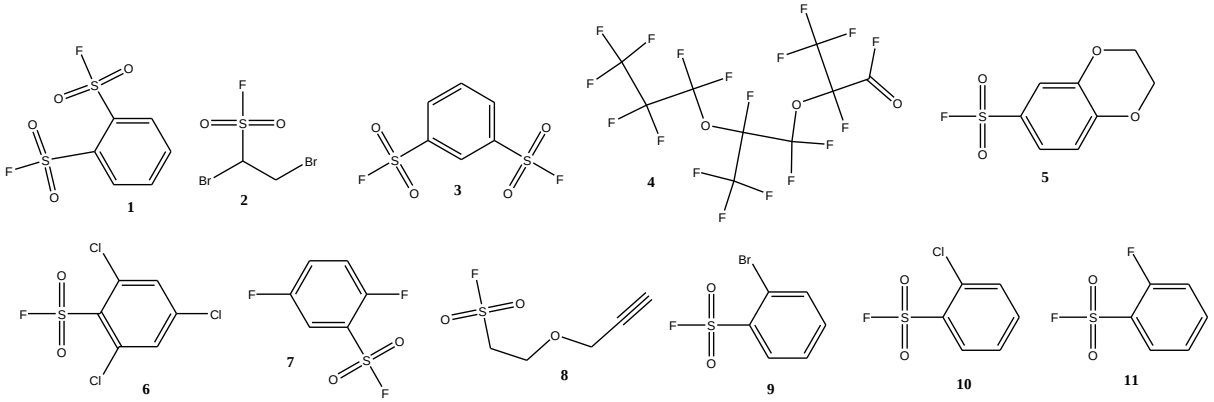

Figure 1. Chemical structure of fluoride derivatives (1-11).

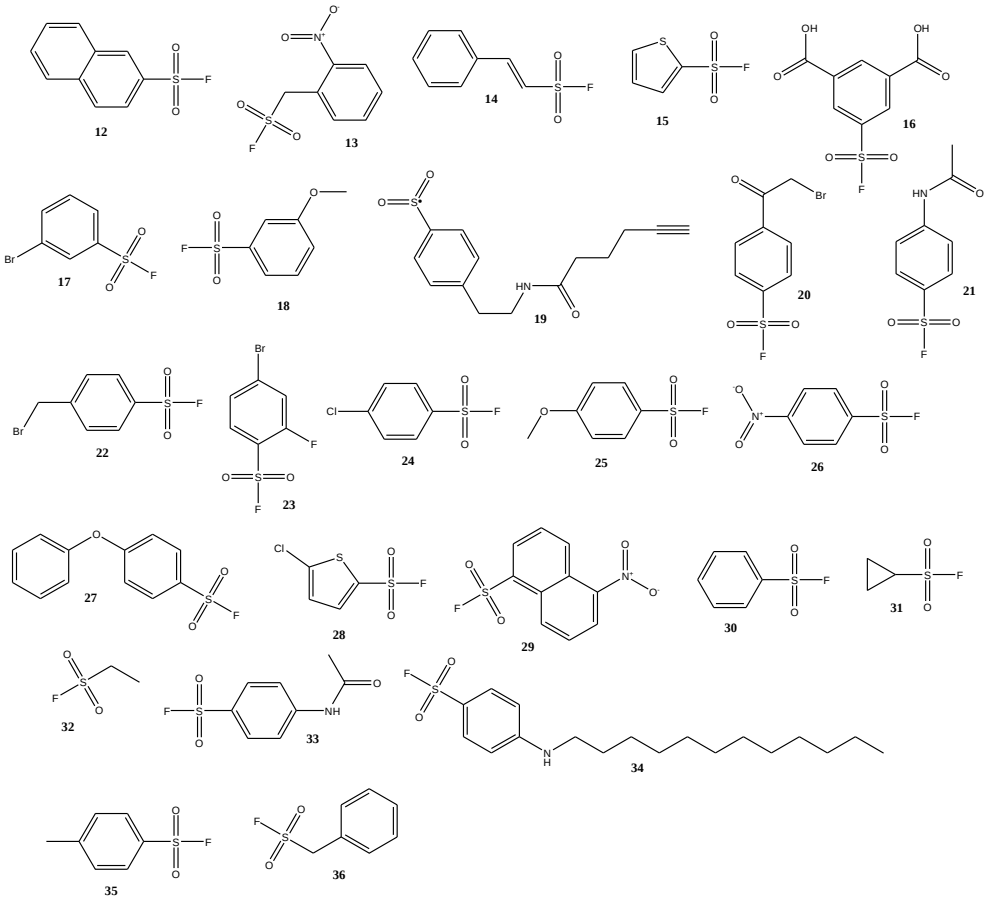

Figure 2. Chemical structure of fluoride derivatives (12-36).

Table 1. Name of fluoride derivatives (1-36).

Comp	Name	Smile
1	Benzene-1,2-disulfonyl fluoride	FS(=O)(=O)c1ccccc1S(=O)(=O)F
2	1,2-Dibromoethane-1-sulfonyl fluoride	FS(=O)(=O)C(Br)CBr
3	1,3-Benzenedisulfonyl fluoride	C1=CC(=CC(=C1)S(=O)(=O)F)S(=O)(=O)F
4	2,3,3,3-tetrafluoro-2-[1,1,2,3,3,3-hexafluo- ro-2-(1,1,2,2,3,3,3-heptafluoropropoxy) propoxy]propanoyl fluoride	FC(=O)C(F)(OC(F)(F)C(F)(OC(F)(F)C(F)(F)C(F)(F)F)C(F)(F)F)C(F)(F)F
5	2,3-Dihydro-1,4-benzodioxine-6-sulfonyl fluoride	FS(=O)(=O)c1ccc2OCCOc2c1
6	2,4,6-Trichloro-benzenesulfonyl fluoride	C1=C(C=C(C(=C1Cl)S(=O)(=O)N)Cl)Cl
7	2,5-Difluoro-benzenesulfonyl fluoride	C1=CC(=C(C=C1F)S(=O)(=O)F)F
8	2-prop-2-ynoxyethanesulfonyl fluoride	FS(=O)(=O)CCOCC#C
9	2-Bromobenzenesulfonyl fluoride	C1=CC=C(C(=C1)S(=O)(=O)F)Br
10	2-Chlorobenzenesulfonyl fluoride	C1=CC(=C(C=C1CBr)S(=O)(=O)F)Cl
11	2-Fluorobenzenesulfonyl fluoride	C1=CC(=C(C=C1Cl)S(=O)(=O)F)F
12	Naphthalene-2-sulfonyl fluoride	C1=CC=C2C=C(C=CC2=C1)S(=O)(=O)F FS(=O)(=O)c1ccc2ccccc2c1
13	(2-nitrophenyl)methanesulfonyl fluoride	[O-][N+](=O)c1ccccc1CS(=O)(=O)F
14	(*E*)-2-phenylethenesulfonyl fluoride	FS(=O)(=O)\C=C\c1ccccc1
15	Thiophene-2-sulfonyl fluoride	FS(=O)(=O)c1cccs1
16	5-fluorosulfonylbenzene-1,3-dicarboxylic acid	OC(=O)c1cc(cc(c1)S(=O)(=O)F)C(=O)O
17	3-Bromobenzenesulfonyl fluoride	C1=CC(=CC(=C1)Br)S(=O)(=O)F
18	3-Methoxybenzenesulfonyl fluoride	COC1=CC(=CC=C1)S(=O)(=O)F
19	N-[2-[4-(dioxo-λ⁵-sulfanyl)phenyl]ethyl] hex-5-ynamide	O=C(CCCC#C)NCCc1ccc(cc1)[S](=O)=O
20	4-(2-Bromoacetyl)benzenesulfonyl fluoride	FS(=O)(=O)c1ccc(cc1)C(=O)CBr
21	4-acetamidobenzenesulfonyl fluoride	CC(=O)Nc1ccc(cc1)S(=O)(=O)F
22	4-(Bromomethyl)benzenesulfonyl fluoride	FS(=O)(=O)c1ccc(CBr)cc1
23	4-bromo-2-fluoro-benzenesulfonyl fluoride	Fc1cc(Br)ccc1S(=O)(=O)F
24	4-Chlorobenzenesulfonyl fluoride	FS(=O)(=O)c1ccc(Cl)cc1
25	4-Methoxybenzenesulfonyl fluoride	COc1ccc(cc1)S(=O)(=O)F
26	4-Nitrobenzenesulfonyl fluoride	[O-][N+](=O)c1ccc(cc1)S(=O)(=O)F
27	4-Phenoxybenzenesulfonyl fluoride	FS(=O)(=O)c1ccc(Oc2ccccc2)cc1

Comp	Name	Smile
28	5-Chlorothiophene-2-sulfonyl fluoride	FS(=O)(=O)c1ccc(Cl)s1
29	5-Nitronaphthalene-1-sulfonyl fluoride	[O-][N+](=O)c1cccc2c(cccc12)S(=O)(=O)F
30	Benzenesulfonyl fluoride	FS(=O)(=O)c1ccccc1
31	Cyclopropanesulfonyl fluoride	FS(=O)(=O)C1CC1
32	Ethanesulfonyl fluoride	CCS(=O)(=O)F
33	4-Acetamidobenzenesulfonyl fluoride	CC(=O)Nc1ccc(cc1)S(=O)(=O)F
34	4-(Dodecylamino)benzenesulfonyl fluoride	CCCCCCCCCCCCNc1ccc(cc1)S(=O)(=O)F
35	p-Toluenesulfonyl fluoride	Cc1ccc(cc1)S(=O)(=O)F
36	Phenylmethanesulfonyl fluoride	FS(=O)(=O)Cc1ccccc1

2.2. Ligand-protein complex.

The coupling of fluoride derivatives (1-36) with EphB4 was determined using the 2VWX protein (https://doi.org/10.2210/pdb2VWX/pdb) [32]. Besides, the 3HNG protein (https://doi.org/10.2210/pdb3HNG/pdb) was used for coupling the fluoride derivatives with VEGFR-1 (Figure 3). It is important to mention that the A chain of each protein was used to predict its coupling with fluoride analogs.

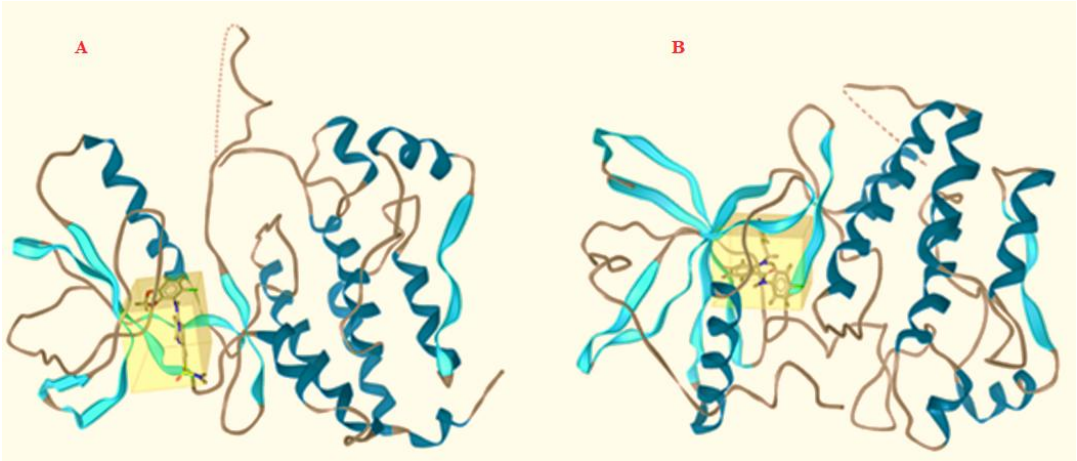

Figure 3. (A) shows the ephB4 domain inhibitor complex with a 3,5-Bis substituted anilinopyrimidine (2VWX protein); **(B)** displays crystal structure of VEGFR1 in complex with N-(4-Chlorophenyl)-2-((pyridin-4-ylmethyl)amino)benzamide (3HNG protein)

It was interesting to use the proteins involved in this study due to the chemical characteristics of the compounds used to select the molecules most likely to show binding and inhibition activity, and compare them with the controls such as sanguinarine, NVP-BHG712 (4-methyl-3-[(1-methyl-6-pyridin-3-ylpyrazolo[3,4-d]pyrimidin-4-yl)amino]-N-[3-(trifluoromethyl)phenyl]benzamide), QDAU5 (1-(3,4-difluorophenyl)-3-(4-(4-oxo-3,4-dihydroquinazolin-7-yl) phenyl)urea), and VDAU-11 (N-(5-(4-(3-(3-chlorophenyl)ureido) phenyl)pyridine-2-yl) acrylamide) in DockingServer software [https://www.dockingserver.com]. Docking calculations were carried out on a ligand-protein model [33]. It is important to note that essential hydrogen atoms, Kollman united-atom type charges, solvation parameters, and the Affinity (grid) maps were generated using the Autogrid program [34]. In addition, AutoDock parameter-set- and distance-dependent dielectric functions were used to determine van der Waals forces and electrostatic factors.

On the other hand, docking simulations were performed using the Lamarckian genetic algorithm and the Solis & Wets method [35]. It is noteworthy that the initial position, orientation, and torsions of the ligand molecules were set randomly. All rotatable torsions were released during docking. Each docking experiment was derived from 2 runs, each set to terminate after a maximum of 250000 energy evaluations. Finally, the population size was set

to 150. During the search, a translational step of 0.2 Å and quaternion and torsion steps of 5 were applied.

2.3. Pharmacokinetic parameters.

Pharmacokinetic factors for fluoride derivatives 6, 10, 12, 27, and 29 were determined using the SwissADME software [36]. The SwissADME program is a theoretical tool used to evaluate the pharmacokinetics, pharmacological similarity, and chemical compatibility of small molecules.

2.4. Toxicology analysis.

Toxicology evaluation for fluoride derivatives 6, 10, 12, 27, and 29 was determined using the Gussar software [37]. It is important to note that the GUSAR program was developed to build models based on the association between chemical structure and the toxicological activity of various drugs. The training sets were created based on data from the SYMYX MDL Toxicity Database. They include information about ~10,000 chemical structures, with data on acute rat toxicity represented by LD50 values (log10 (mmol/kg)).

3. Results and Discussion

3.1. First stage.

3.1.1. Fluoride-2vwx complex.

The interaction of fluoride derivatives with EPHB4 was determined using the 2vwx protein as a theoretical tool in the DockingServer program. The results (Table 2) showed differences in the amino acid residues involved in the coupling of fluoride derivatives with 2VWX compared with those with sanguinarine, NVP-VBG712, and VDAU-11 drugs.

Table 2. Amino acid residues involved in the coupling of fluoride derivatives (1-36) with the 2vwx protein surface.

Compounds	Aminoacid residues
Sanguinarine	Ile_{621}; Ala_{645}; Lys_{647}; Ile_{677}; Thr_{693}; Phe_{695}; Met_{696}; Leu_{747}
NVPBHG712	Ile_{621}; Ala_{623}; Val_{629}; Ala_{645}; Lys_{647}; Glu_{664}; Met_{668}; Ile_{677}; Thr_{693}; Ala_{700}; Arg_{744}; Asn_{745}; Leu_{747}; Ser_{757}; Asp_{758}
VDAU-11	Ile_{621}; Val_{629}; Arg_{631}; Ala_{645}; Lys_{647}; Phe_{695}; Met_{696}; Glu_{697}; Leu_{747}
QDAU5	Ile_{621}; Val_{629}; Ala_{645}; Lys_{647}; Glu_{664}; Met_{668}; Ile_{691}; Thr_{693}; Phe_{695}; Met_{696}; Glu_{697}; Asn_{698}; Leu_{747}; Ser_{757}
1	Val_{629}; Ala_{645}; Lys_{647}; Glu_{664}; Met_{668}; Ile_{677}; Ile_{691}; Thr_{693}; Leu_{747}
2	Ala_{645}; Lys_{647}; Glu_{664}; Met_{668}; Ile_{677}; Ile_{691}; Thr_{693}; Leu_{747}; Ser_{757}
3	Ile_{621}; Val_{629}; Ala_{645}; Lys_{647}; Ile_{677}; Ile_{691}; Thr_{693}; Phe_{695}; Met_{696}; Leu_{747}; Ser_{757}
4	Val_{629}; Ala_{645}; Ile_{646}; Lys_{647}; Glu_{664}; Met_{668}; Thr_{693}; Arg_{744}; Asn_{745}; Leu_{747}; Ser_{757}; Asp_{758}
5	Ile_{621}; Ala_{645}; Lys_{647}; Glu_{664}; Thr_{693}; Glu_{694}; Phe_{695}; Met_{696}; Leu_{747}
6	Val_{629}; Ala_{645}; Glu_{664}; Met_{668}; Ile_{691}; Thr_{693}; Leu_{747}; Ser_{757}
7	Ala_{645}; Lys_{647}; Glu_{664}; Met_{668}; Ile_{677}; Ile_{691}; Thr_{693}; Leu_{747}; Ser_{757}
8	Ile_{621}; Val_{629}; Ala_{645}; Thr_{693}; Glu_{694}; Phe_{695}; Met_{696}; Leu_{747}
9	Lys_{647}; Glu_{664}; Met_{668}; Ile_{677}; Ile_{691}; Thr_{693}; Leu_{747}; Ser_{757}
10	Ala_{645}; Lys_{647}; Glu_{664}; Met_{668}; Ile_{677}; Ile_{691}; Thr_{693}; Leu_{747}
11	Ala_{645}; Lys_{647}; Glu_{664}; Met_{668}; Ile_{677}; Ile_{691}; Thr_{693}; Leu_{747}
12	Ile_{621}; Val_{629}; Ala_{645}; Ile_{677}; Thr_{693}; Phe_{695}; Met_{696}; Leu_{747}; Ser_{757}
13	Val_{629}; Ala_{645}; Lys_{647}; Glu_{664}; Met_{668}; Thr_{693}; Leu_{747}
14	Ile_{621}; Val_{629}; Ala_{645}; Glu_{664}; Met_{668}; Ile_{677}; Ile_{691}; Thr_{693}; Glu_{694}; Phe_{695}; Met_{696}; Leu_{747}; Ser_{757}
15	Ala_{645}; Lys_{647}; Met_{668}; Ile_{677}; Ile_{691}; Thr_{693}; Leu_{747}
16	Ile_{621}; Val_{629}; Ala_{645}; Lys_{647}; Thr_{693}; Glu_{694}; Phe_{695}; Met_{696}; Leu_{747}
17	Ile_{621}; Val_{629}; Ala_{645}; Lys_{647}; Thr_{693}; Met_{696}; Leu_{747}
18	Ile_{621}; Val_{629}; Ala_{645}; Ile_{677}; Thr_{693}; Phe_{695}; Met_{696}; Leu_{747}
19	Ile_{621}; Val_{629}; Ala_{645}; Lys_{647}; Glu_{664}; Met_{668}; Ile_{677}; Thr_{693}; Phe_{695}; Met_{696}; Leu_{747}; Ser_{757}

Compounds	Aminoacid residues
20	Ile621; Val629; Ala645; Lys647; Glu664; Met668; Ile677; Thr693; Phe695; Met696; Leu747; Ser757
21	Ile621; Val629; Ala645; Met668; Thr693; Phe695; Met696; Leu747
22	Ile621; Val629; Ala645; Lys647; Thr693; Phe695; Met696; Leu747
23	Ile621; Ala645; Ile677; Thr693; Glu694; Phe695; Met696; Leu747
24	Ile621; Val629; Ala645; Ile677; Thr693; Phe695; Met696; Leu747
25	Ile621; Val629; Ala645; Lys647; Thr693; Glu694; Phe695; Met696; Leu747
26	Ile621; Val629; Ala645; Lys647; Glu664; Met668; Ile691; Thr693; Met696; Leu747
27	Ala645; Lys647; Glu664; Met668; Ile691; Thr693; Arg744; Asn745; Leu747; Ser757
28	Ile621; Val629; Ala645; Ile677; Thr693; Phe695; Met696; Leu747
29	Ile621; Val629; Ala645; Lys647; Thr693; Phe695; Met696; Leu747; Ser757
30	Ala645; Lys647; Met668; Ile677; Ile691; Thr693; Leu747; Ser757
31	Val629; Ala645; Phe695; Met696; Leu747
32	Ile621; Val629; Ala645; Thr693; Phe695; Met696; Leu747
33	Ile621; Ala645; Lys647; Glu664; Thr693; Phe695; Met696; Leu747
34	Ile621; Val629; Arg631; Ala645; Lys647; Thr693; Phe695; Met696; Leu747
35	Ala645; Ile677; Thr693; Met696; Leu747
36	Val629; Ala645; Lys647; Ile691; Thr693; Leu747

3.1.2. Thermodynamic parameters.

Table 3 shows the energy levels and inhibition constant (Ki) involved in the interaction of fluoride derivatives (1-36) with the 2vwx protein surface. The results indicate differences in the energy levels and Ki for fluoride derivatives compared with the controls.

Table 3. Thermodynamic parameters involved in the interaction of fluoride derivatives (1-36) with the 2VWX protein surface.

Compound	A	B	C	D	E	F
Sanguinarine	-7.28	4.64	-6.94	-0.34	-7.28	696.60
NVPBHG712	-8.22	0.943	-9.50	-0.13	-9.63	989.66
VDAU-11	-6.65	13.25	-7.89	0.00	-7.23	848.75
QDAU5	-843	0.660	-9,23	-0.13	-9.36	759.59
1	-5.32	126.86	-5.94	0.12	-5.92	441.61
2	-3.75	1780	-4.22	-0.08	-4.29	298.62
3	-5.42	106.84	-6.02	0.00	-6.01	481.10
4	-5.24	143.10	-8.42	-0.03	-8.45	545.90
5	-4.59	428.60	-4.60	-0.09	-4.89	497.88
6	-6.12	32.86	-6.50	0.09	-6.41	488.10
7	-5.35	119.88	-5.77	0.13	-5.85	386.16
8	-3.62	2210	-5.01	-0.01	-5.02	441.62
9	-5.04	203.59	-5.33	0.00	-5.33	383.20
10	-5.86	50.84	-6.18	0.03	-6.16	418.90
11	-5.11	178.46	-5.47	0.06	-5.41	390.45
12	-5.67	69.41	-5.96	-0.02	-5.97	515.68
13	-5.38	113.13	-6.18	0.02	-6.16	476.14
14	-5.02	209.03	-5.60	-0.01	-5.61	478.44
15	-4.95	233.94	-5.27	0.02	-5.25	350.70
16	-4.22	808.69	-5.33	0.41	-5.11	524.47
17	-4.80	304.73	-5.09	-0.01	-5.10	432.22
18	-4.59	428.77	-5.15	-0.04	-5.19	472.01
19	-5.07	191.07	-6.87	0.11	-6.77	675.65
20	-4.97	227.85	-5.69	-0.02	-5.71	496.70
21	-4.67	374.54	-5.24	0.00	-5.23	524.32
22	-4.83	286.8	-5.44	0.01	-5.43	458.99
23	-5.14	170.48	-5.46	0.02	-5.44	405.60
24	-5.22	149.60	-5.53	0.01	-5.52	470.44
25	-4.43	569.84	-5.03	0.01	-5.02	463.21
26	-4.94	240.36	-5.57	0.04	-5.53	449.35
27	-5.23	147.28	-6.27	0.11	-6.15	541.71
28	-5.30	130.17	-5.60	0.00	-5.60	447.24
29	-5.62	76.38	-6.33	0.05	-6.28	543.45
30	-5.00	217.88	-5.31	0.01	-5.29	381.12
31	-3.48	2810	-3.75	-0.03	-3.78	302.16
32	-3.32	3670	-3.61	-0.01	-3.62	272.30
33	-4.80	302.07	-5.43	0.05	-5.36	525.26

Compound	A	B	C	D	E	F
34	-5.93	44.71	-9.41	0.00	-9.41	734.60
35	-4.71	351.28	-4.99	-0.02	-5.01	471.91
36	-4.53	478.97	-5.16	0.01	-5.15	428.24

A = Est: Free Energy of Binding (kcal/mol); B = Inhibition Constant (Ki, μM); C = vdW + Hbond + desolv Energy (kcal/mol); D = Electrostatic Energy (kcal/mol); E = Total Intermolec. Energy (kcal/mol); F= Interact. Surface.

3.1.3. Bond type.

Figures 4-6 and Table 4 show differences in the types of bonds involved in the coupling of fluoride derivatives (6 and 10) with the 2vwx protein surface. Furthermore, Table 5 shows the decomposed interaction energies involved for fluoride derivatives 6 and 10.

Table 4. Bond type and distance (nm) levels involved in the interaction of fluoride derivatives (6 and 10) and the controls with the 2vwx protein surface.

Comp.	Hydrogen bond	Polar Bond	Hydrophobic bond	pi-pi	Halogen bond
Sanguinarine	Thr_{693} (C_2, 3.30)		Ile_{621} (C_{12}, 3.60) Ile_{621} (C_{13}, 3.46) Ile_{621} (C_{14}, 3.63) Ile_{621} (C_{15}, 3.88) Ile_{621} (C_{18}, 3.86) Ala_{645} (C_8, 3.73) Ala_{645} (C_9, 3.62) Met_{696} (C_9, 3.73) Met_{696} (C_{10}, 3.70) Leu_{747} (C_1, 3.75) Leu_{747} (C_2, 3.51) Leu_{747} (C_3, 3.88) Leu_{747} (C_6, 3.69) Leu_{747} (C_7, 3.37) Leu_{747} (C_8, 3.27) Leu_{747} (C_9, 3.83) Leu_{747} (C_{20}, 3.74)	Phe_{695} (C_{13}, 3.33) Phe_{695} (C_{14}, 3.85)	
NVPBHG712	Glu_{664} (N_6, 2.65) Glu_{664} (N_5, 3.18) Arg_{744} (N_3, 3.40) Asn_{745} (N_2, 3.43) Asn_{745} (N_3, 3.47) Asp_{758} (N_5, 3.37) Glu_{664} (H_6, 3.20) Ser_{757} (H_6, 3.85)	Lys_{647} (N_6, 3.75) Lys_{647} (N_4, 3.82) Lys_{647} (N_5, 3.05) Arg_{744} (N_1, 3.22) Asp_{758} (N_4, 3.59)	Ile_{621} (C_{22}, 3.12) Ile_{621} (C_{23}, 3.82) Val_{629} (C_{20}, 3.61) Val_{629} (C_{21}, 3.26) Val_{629} (C_{22}, 3.48) Met_{668} (C_{17}, 3.14) Ile_{677} (C_{15}, 3.37) Ala_{700} (C_{20}, 3.84) Leu_{747} (C_{14}, 3.86)		Ile_{621} (F_1, 3.50) Ala_{623} (F_3, 3.62)
VDAU-11	Met_{696} (N_2, 2.95) Glu_{697} (N_2, 3.42) Glu_{697} (N_1, 2.75)	Ser_{757} (N_4, 3.72) Ser_{757} (H_{13}, 2.81)	Ile_{621} (C_7, 3.50) Ile_{621} (C_6, 3.86) Ile_{621} (C_8, 3.38) Val_{629} (C_{13}, 3.35) Val_{629} (C_{14}, 3.54) Ala_{700} (C_{18}, 3.60) Ala_{700} (C_{19}, 3.62) Leu_{747} (C_{11}, 3.23) Leu_{747} (C_{10}, 3.39) Leu_{747} (C_{17}, 3.64)	Phe_{695} (C_8, 3.45)	
QDAU5	Glu_{664} (N_4, 2.74) Met_{696} (N_2, 2.75) Glu_{697} (N_1, 2.77)	Lys_{647} (N_4, 3.37) Lys_{647} (H_8, 3.27) Glu_{664} (H_8, 1.74) Glu_{664} (O_2, 3.44)	Ile_{621} (C_2, 3.65) Ile_{621} (C_7, 3.29) Ile_{621} (C_1, 3.64) Ala_{645} (C_6, 3.14) Ala_{645} (C_7, 3.80) Ala_{645} (C_{12}, 3.74) Leu_{747} (C_4, 3.08) Leu_{747} (C_{13}, 3.39) Leu_{747} (C_{12}, 3.77) Leu_{747} (C_{15}, 3.81) Leu_{747} (C_{14}, 3.41) Leu_{747} (C_3, 3.77)	Phe_{695} (C_7, 3.24) Phe_{695} (C_2, 3.66)	

Comp.	Hydrogen bond	Polar Bond	Hydrophobic bond	pi-pi	Halogen bond
6	Ser_{757} (O, 3.18)	Glu_{664} (O, 3.60)			Ala_{645} Cl, 3,66) Glu_{664} (Br, 3.44) Ile_{691} (Cl, 3.36) Thr_{693} (Cl, 3.55) Ser_{757} (F, 2.89)
10			Ala_{645} (C_6, 3.29) Met_{688} (C_3, 3.89) Ile_{691} (C_4, 3.31) Ile_{691} (C_3, 3.48)		Glu_{664} (Cl, 3.51) Thr_{693} (F, 3.00)

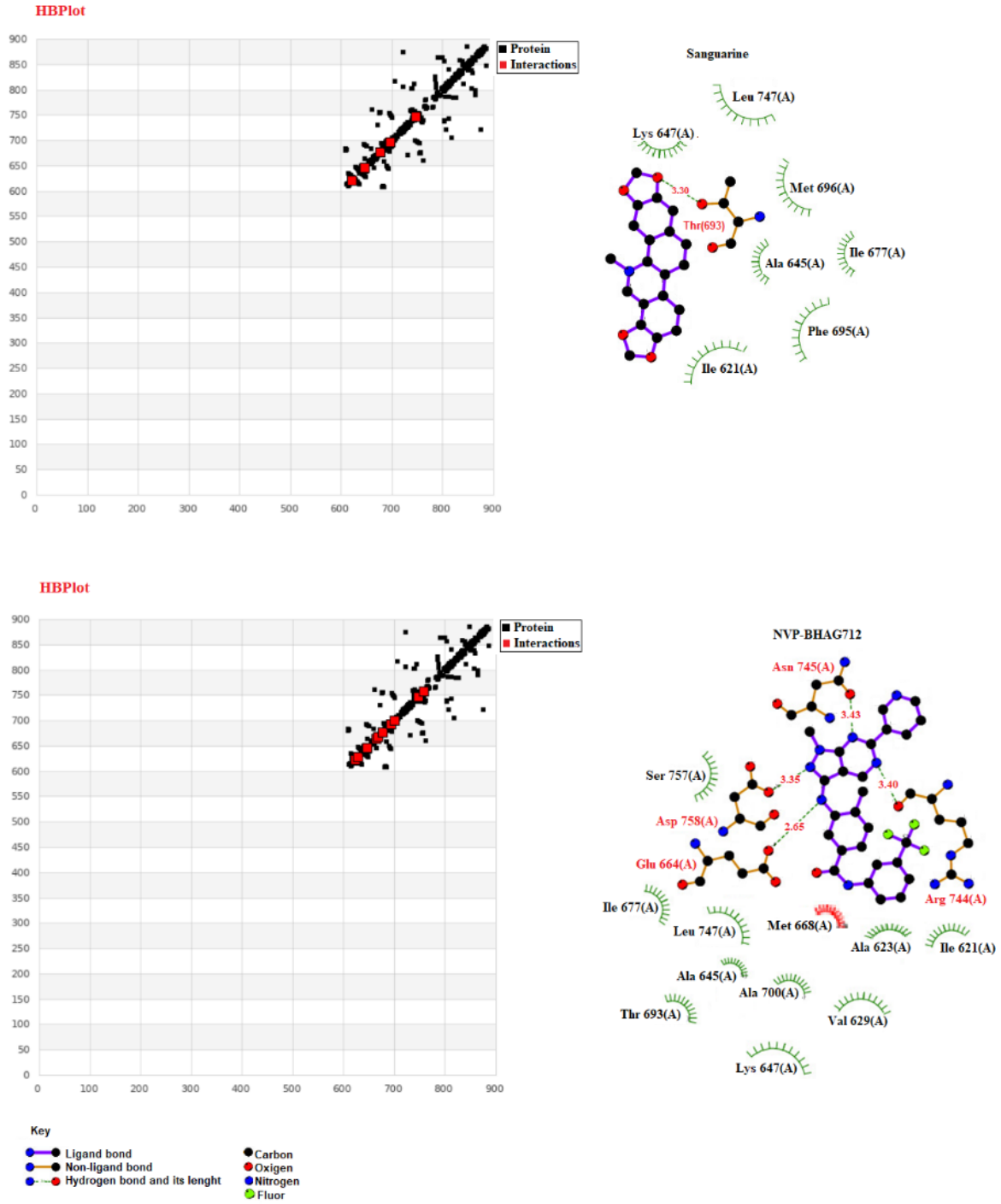

Figure 4. The scheme shows the ligand-protein complex formation between Sanguinarine and NVP-BHAG712 drugs with the 2VWX protein surface. Visualized with the DockingServer program.

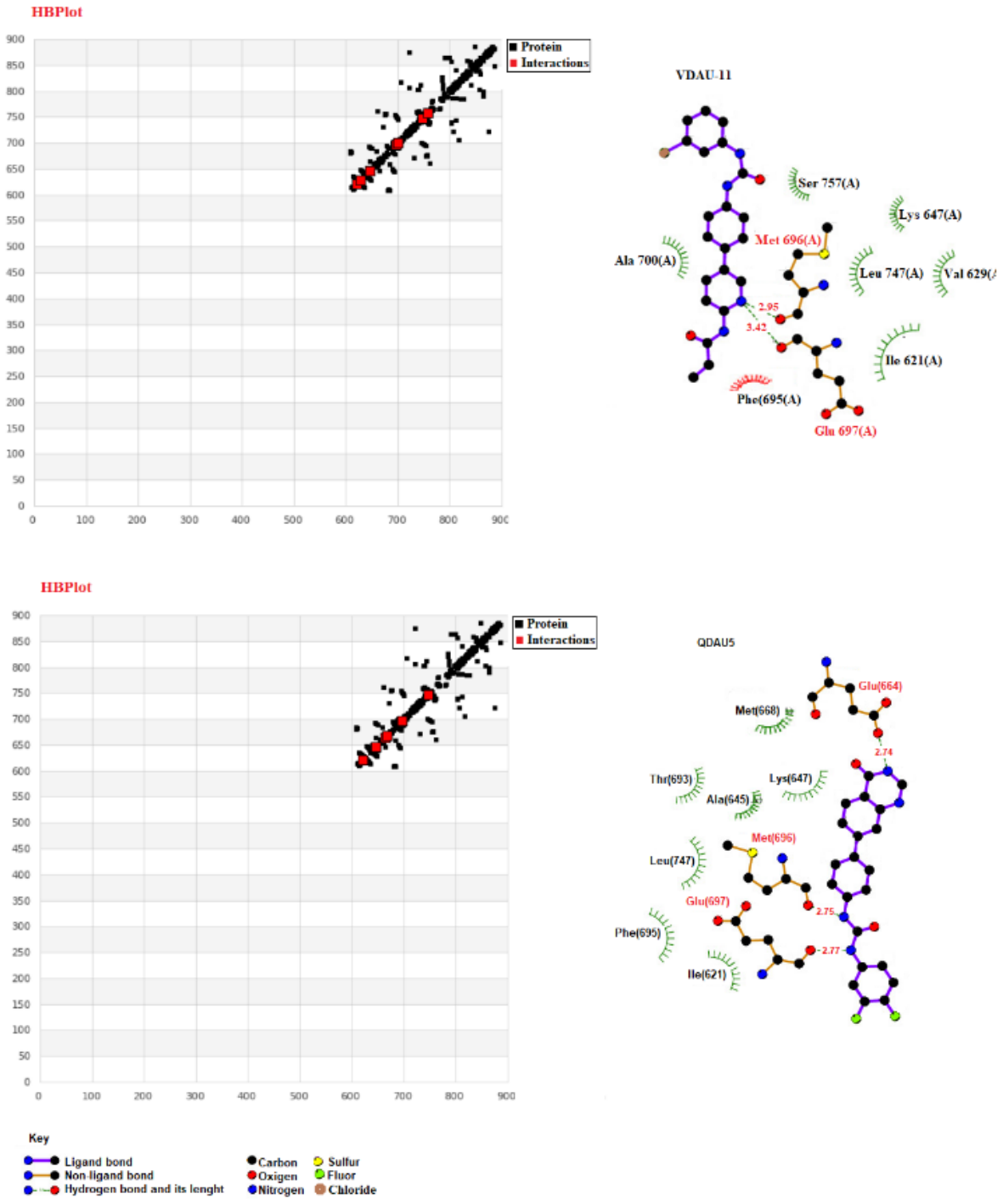

Figure 5. The scheme displays the coupling of VDAU-11 and QDAU5 drugs with the 2VWX protein surface. Visualized with the DockingServer program.

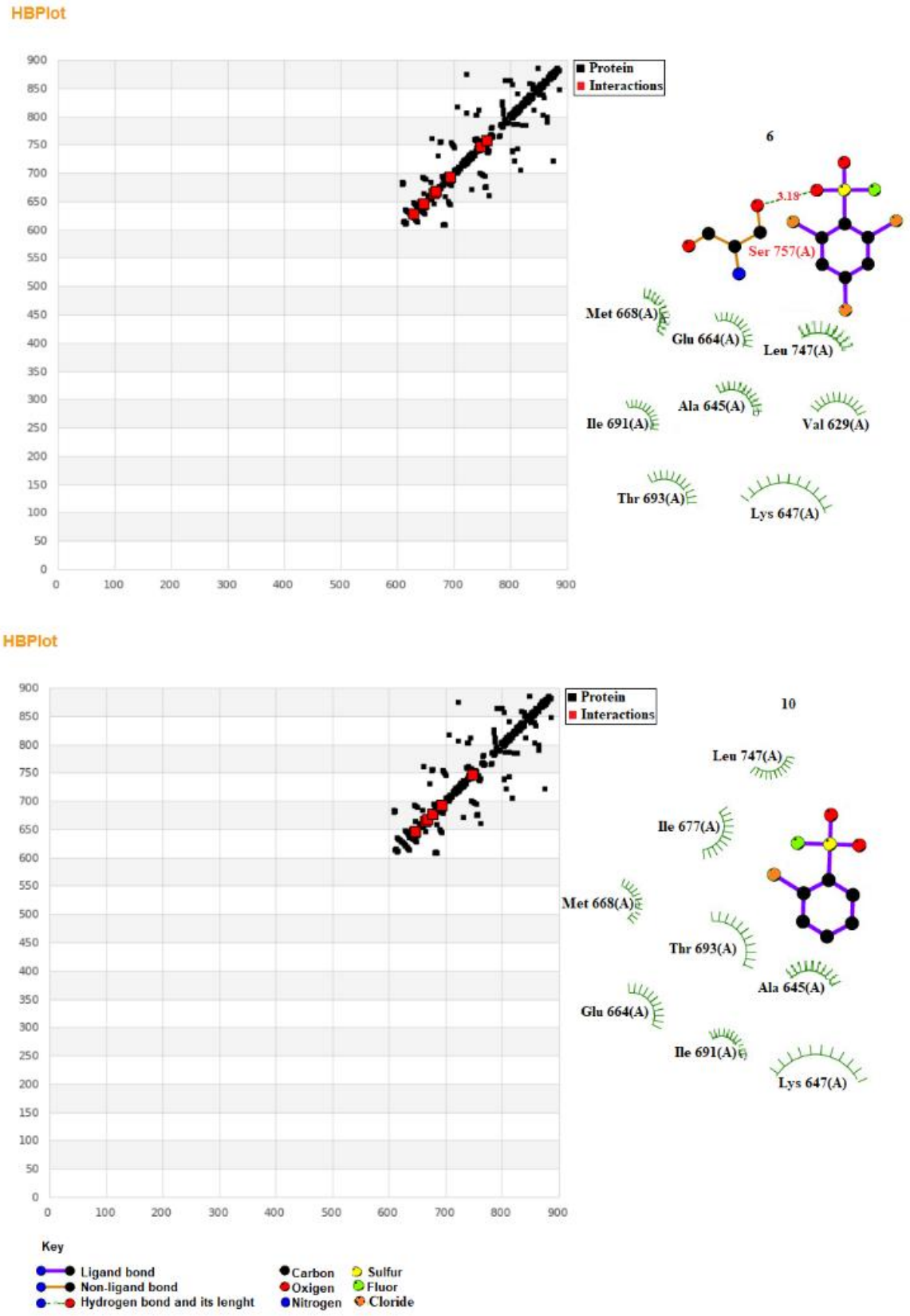

Figure 6. Coupling of fluoride derivatives 6 and 10 with the 2VWXprotein surface. Visualized with the DockingServer program.

Table 5. Decomposed interaction energies in kcal/mol involved in the coupling of Sanguinarine, QDAU5, NVP-BHG712, VDAU-11, and fluoride derivatives (6 and 10) with the 2VWX protein surface.

Compound	Hydrogen bond	Polar Bond	Hydrophobic bond	Halogen bond
Sanguinarine	Thr_{693} (-0.424)		Ile_{621} (-1.181) Leu_{747} (-1.159) Phe_{695} (-1.130)	

Compound	Hydrogen bond	Polar Bond	Hydrophobic bond	Halogen bond
			Met_{696} (-0.939) Ala_{645} (-0.473)	
QDAU5	Met_{696} (-1.194) Glu_{664} (-0.645) Glu_{697} (-0.379)	Lys_{647} (-0.727)	Leu_{747} (-0.795) Ile_{621} (-0.654) Ala_{645} (-0.135)	
NVP-BHG712	Asp_{758} (-1.415) Asn_{745} (-1.048) Arg_{744} (-0.589) Glu_{664} (-0.516)	Lys_{647} (-1.342)	Val_{629} (-0.972) Leu_{747} (-0.955) Ile_{677} (-0.580) Ala_{700} (-0.428) Met_{668} (0.006)	Ile_{621} (-0.647) Ala_{623} (-0.341)
VDAU-11	Glu_{697} (-0.899) Met_{696} (0.166)	Ser_{757} (-0.353)	Ile_{621} (-1.418) Leu_{747} (-0.780) Val_{629} (-0.685) Ala_{700} (-0.628) Phe_{695} (0.149)	
6	Ser_{757} (-0.2901)			Thr_{693} (-6217) Glu_{664} (-0.4546) Ile_{691} (-0.3194) Ala_{645} (-2638)
10			Met_{668} (-0.2481) Ala_{645} (-0.2344) Ile_{691} (-0.0908)	Thr_{693} (-0.6777) Glu_{694} (-0.3995)

3.2. Second stage.

3.2.1. Fluoride-3hng complex.

Table 6 shows differences in amino acid residues involved in the coupling of fluoride derivatives with the 3HNG protein surface compared with sanguinarine, NVP-VHG712, QDAU5, and VDAU-11 drugs.

Table 6. Amino acid residues involved in the coupling of fluoride derivatives (1-36) with the 3HNG protein surface.

Compounds	Aminoacid residues
Sanguinarine	Asp_{807}; Glu_{878}; Leu_{882}; Val_{891}; Val_{892}; His_{102}; Arg_{1021}; Asp_{1040}
NVP-VHG712	Val_{841}; Ala_{859}; Lys_{861}; Glu_{878}; Ile_{881}; Leu_{882}; Ile_{885}; Val_{907}; Val_{909}; Cys_{918}; Ile_{1019}; His_{1020}; Arg_{1021}; Cys_{1039}; Asp_{1040}; Leu_{1043}
VDAU1-11	Val_{841}; Ala_{859}; Lys_{861}; Glu_{878}; Ile_{881}; Val_{892}; Cys_{1018}; Ile_{1019}; His_{1020}; Arg_{1021}; Cys_{1018}; Cys_{1039}; Asp_{1040}
QDAU5	Leu_{833}; Ala_{859}; Lys_{861}; Glu_{878}; Ile_{881}; Leu_{882}; Val_{892}; Val_{909}; Cys_{1039}; Asp_{1040}; Phe_{1041}
1	Val_{841}; Ala_{859}; Lys_{861}; Glu_{878}; Val_{892}; Val_{909}; Leu_{1029}; Cys_{1039}; Asp_{1040}; Phe_{1041}
2	Val_{841}; Ala_{859}; Lys_{861}; Val_{892}; Val_{909}; Glu_{910}; Leu_{1029}; Cys_{1039}; Asp_{1040}; Phe_{1041}
3	Leu_{833}; Ala_{859}; Lys_{861}; Val_{892}; Val_{909}; Tyr_{911}; Cys_{912}; Leu_{1029}; Cys_{1039}; Asp_{1040}; Phe_{1041}
4	Glu_{878}; Ile_{881}; Leu_{882}; Ile_{885}; Val_{891}; Val_{892}; Val_{909}; Leu_{1013}; Cys_{1018}; His_{1020}; Ile_{1038}; Cys_{1039}; Asp_{1040}
5	Leu_{833}; Lys_{861}; Val_{892}; Val_{909}; Cys_{912}; Leu_{1029}; Cys_{1039}; Asp_{1040}; Phe_{1041}
6	Glu_{878}; Ile_{881}; Val_{891}; Leu_{1013}; Cys_{1018}; His_{1020}; Ile_{1038} ; Asp_{1040}
7	Val_{841}; Lys_{861}; Glu_{878}; Leu_{882}; Val_{907}; Val_{909}; Leu_{1029}; Cys_{1039}; Asp_{1040}; Phe_{1041}
8	Val_{841}; Ala_{859}; Lys_{861}; Glu_{878}; Val_{907}; Val_{909}; Leu_{1029}; Cys_{1039}; Asp_{1040}; Phe_{1041}
9	Val_{841}; Ala_{859}; Lys_{861}; Glu_{878}; Val_{892}; Val_{907}; Val_{909}; Leu_{1029}; Cys_{1039}; Asp_{1040}
10	Val_{841}; Lys_{861}; Glu_{878}; Val_{892}; Val_{909}; Leu_{1029}; Cys_{1039}; Asp_{1040}; Phe_{1041}
11	Val_{841}; Ala_{859}; Lys_{861}; Glu_{878}; Val_{892}; Val_{907}; Val_{909}; Cys_{1039}; Asp_{1040}
12	Leu_{833}; Val_{841}; Ala_{859}; Lys_{861}; Val_{892}; Val_{909}; Tyr_{911}; Cys_{912}; Leu_{1029}; Cys_{1039}; Asp_{1040}; Phe_{1041}
13	Val_{841}; Ala_{859}; Lys_{861}; Glu_{878}; Val_{892}; Val_{907}; Val_{909}; Leu_{1029}; Cys_{1039}; Asp_{1040}
14	Leu_{833}; Val_{841}; Ala_{859}; Lys_{861}; Val_{909}; Tyr_{911}; Cys_{1039}; Asp_{1040}; Phe_{1041}
15	Val_{841}; Lys_{861}; Glu_{878}; Val_{892}; Val_{907}; Val_{909}; Cys_{1039}; Asp_{1040}
16	Lys_{861}; Glu_{878}; Leu_{882}; Val_{892}; Val_{907}; Val_{909}; Leu_{1029}; Cys_{1039}; Asp_{1040}
17	Val_{841}; Ala_{859}; Lys_{861}; Glu_{878}; Val_{892}; Val_{907}; Val_{909}; Leu_{1029}; Cys_{1039}; Asp_{1040}; Phe_{1041}
18	Leu_{833}; Val_{841}; Ala_{859}; Lys_{861}; Val_{892}; Val_{909}; Tyr_{911}; Leu_{1029}; Cys_{1039}; Asp_{1040}
19	Ala_{859}; Lys_{861}; Glu_{878}; Leu_{882}; Val_{909}; Leu_{1013}; Cys_{1018}; His_{1020}; Leu_{1029}; Cys_{1039}; Asp_{1040}; Phe_{1041}
20	Lys_{861}; Glu_{878}; Leu_{882}; Ile_{885}; Val_{891}; Val_{892}; Val_{909}; Leu_{1013}; His_{1020}; Ile_{1038}; Asp_{1040}
21	Lys_{861}; Glu_{878}; Leu_{882}; Val_{891}; Val_{892}; Val_{909}; Leu_{1013}; His_{1020}; Ile_{1038}; Cys_{1039}; Asp_{1040}
22	Val_{841}; Ala_{859}; Lys_{861}; Val_{891}; Val_{909}; Tyr_{911}; Cys_{912}; Leu_{1029}; Cys_{1039}; Asp_{1040}; Phe_{1041}
23	Leu_{833}; Val_{841}; Ala_{859}; Val_{909}; Glu_{910}; Tyr_{911}; Cys_{912}; Leu_{1029}; Phe_{1041}
24	Lys_{861}; Val_{891}; Val_{909}; Tyr_{911}; Leu_{1029}; Cys_{1039}; Asp_{1040}; Phe_{1041}

Compounds	Aminoacid residues
25	Leu833; Val841; Ala859; Lys861; Val892; Val909; Tyr911; Leu1029; Cys1039; Asp1040
26	Lys861; Glu878; Leu882; Val892; Val909; His1020; Ile1038; Asp1040
27	Val841; Lys861; Glu878; Val891; Val892; His1020; Ile1038; Cys1039; Asp1040; Phe1041
28	Ala859; Lys861; Leu882; Val909; Tyr911; Leu1029; Cys1039; Asp1040; Phe1041
29	Leu833; Val841; Lys861; Glu878; Val892; Val909; Tyr911; Leu1029; Cys1039; Phe1041
30	Val841; Lys861; Glu878; Val892; Val907; Val909; Cys1039; Asp1040; Phe1041
31	Glu878; Val892; Val891; Val892; Cys1039; Asp1040
32	Lys861; Val892; Val909; Cys1039; Asp1040
33	Lys861; Glu878; Leu882; Ile885; Val891; Val892; Val909; His1020; Ile1038; Cys1039; Asp1040
34	Asp807; Glu878; Leu882; Val892; Ile1019; His1020; Arg1021; Tyr911; Cys1039; Asp1040; Phe1041
35	Leu833; Val841; Ala859; Lys861; Val909; Tyr911; Tyr911; Cys1039; Asp1040; Phe1041
36	Leu833; Val841; Ala859; Lys861; Val892; Val909; Leu1029; Cys1039; Asp1040; Phe1041

Table 7 displays the energy levels and inhibition constant (Ki) for the interactions of fluoride derivatives (1-36) with the 3HNG protein surface. The results indicate differences in the energy levels and Ki for fluoride derivatives compared with the controls.

Table 7. Thermodynamic parameters involved in the interaction of fluoride derivatives (1-36) with the 3HNG protein surface.

Compound	A	B	C	D	E	F
Sanguinarine	-7.36	4.05	-6.74	-0.62	-7.36	698.69
NVP-BHG712	-9.74	0.0842	-11.45	-0.07	-11.52	1049.71
VDAU-11	-7.53	3.02	-8.80	-0.05	-8.86	967.60
QDAU5	-8.79	0.0363	-9.68	0.01	-9.67	889.25
1	-6.25	26.05	-6.96	0.01	-6.95	436.98
2	-4.25	761.13	-4.79	-0.02	-4.81	286.70
3	-6.19	29.09	-6.75	-0.03	-6.78	457.62
4	-5.39	111.63	-9.28	0.11	-9.16	592.87
5	-5.86	50.64	-6.08	-0.08	-6.16	486.38
6	-6.90	8.80	-7.20	-0.00	-7.20	526.48
7	-6.15	30.98	-8.40	-0.05	-6.45	397.15
8	-4.09	998.62	-5.54	-0.04	-5.58	399.50
9	-6.10	33.77	-6.37	-0.03	-6.40	380.13
10	-6.54	16.09	-6.84	0.01	-6.84	426.98
11	-5.88	48.58	-6.14	-0.04	-6.18	381.76
12	-6.96	7.97	-7.94	-0.02	-7.25	498.86
13	-6.59	14.71	-7.31	0.01	-7.30	458.59
14	-5.80	55.60	-6.39	-0.01	-6.40	486.97
15	-5.51	92.12	-5.77	-0.03	-5.80	349.10
16	-5.91	46.54	-6.16	-0.64	-6.80	507.67
17	-5.73	63.39	-6.04	0.01	-6.03	388.39
18	-5.30	130.85	-5.87	-0.02	-5.89	469.35
19	-6.68	12.61	-8.88	0.03	-8.85	758.58
20	-6.12	32.40	-6.89	-0.13	-7.02	479.23
21	-6.23	23.01	-6.80	-0.11	-6.91	523.11
22	-5.62	76.53	-6.23	0.00	-6.24	448.59
23	-5.91	46.88	-6.21	0.01	-6.20	402.53
24	-6.10	33.57	-6.38	-0.02	-6.40	454.19
25	-5.30	130.85	-5.87	-0.02	-5.89	439.35
26	-5.89	47.81	-6.45	-0.04	-6.49	459.13
27	-6.96	7.94	-7.90	0.05	-7.85	588.85
28	-6.28	24.98	-6.55	-0.02	-6.58	436.39
29	-7.04	6.86	-7.80	-0.03	-7.77	521.62
30	-5.66	70.42	-5.95	-0.01	-5.96	382.43
31	-3.68	2000	-4.01	0.03	-3.98	299.65
32	-3.39	3300	-3.68	-0.03	-3.98	294.03
33	-6.25	26.18	-6.73	-0.09	-6.81	529.96
34	-6.42	19.56	-9.84	-0.06	-9.91	885.80
35	-5.44	102.92	-6.02	-0.04	-6.05	423.67
36	-5.46	99.02	-6.08	-0.02	-6.11	425.48

A = Est: Free Energy of Binding (kcal/mol); B = Inhibition Constant (Ki, μM); C = vdW + Hbond + desolv Energy (kcal/mol); D = Electrostatic Energy (kcal/mol); E = Total Intermolec. Energy (kcal/mol); F= Interact. Surface.

3.2.2. Bond type.

Figure 7-10 and Table 8 display differences in the types of bonds involved in the interaction of fluoride derivatives (6, 12, 27 and 29) with the 3HNG protein surface. Besides, Table 9 shows the decomposed interaction energies involved for fluoride 6, 12, 27, and 29.

Table 8. Bond type and distance levels involved in the interaction of fluoride derivatives (6, 31, and 32) with the 3HNG protein surface.

Compound	Hydrogen bond	Polar Bond	Hydrophobic bond	Halogen bond
Sanguinarine	Arg_{1021} (O_2, 3.03) Asp_{1040} (N_1, 3.49)	Asp_{1040} (O_2, 3.38)	Leu_{882} (C_{16}, 3.82) Leu_{882} (C_{17}, 3.80) Val_{891} (C_{14}, 3,45) Val_{891} (C_{15}, 3,85) Val_{892} (C_{16}, 3,19) His_{1020} (C_{10}, 3,56)	
VDA-U1-11	Cys_{1018} (O_2, 3.52) Ile_{1019} (N_4, 2.95) His_{1020} (N_4, 3.45)	Arg_{1021} (H_{13}, 3.49) Arg_{1021} (O_2, 3.76)	Ile_{881} (C_{13}, 3.63) Val_{892} (C_2, 3.78) Cys_{1039} (C_4, 3.69) Cys_{1039} (C_1, 3.39) Cys_{1039} (C_2, 3.81)	Glu_{878} (C_{11}, 3.44) Asp_{1040} (C_{11}, 3.58)
NVP-VHG712	Glu_{878} (N_7, 2.94) Glu_{878} (N_1, 2.60) Ile_{1019} (N_6, 3.22) Ile_{1019} (N_5, 2.69) His_{1020} (N_6, 3.3.41) Asp_{1040} (O_1, 3.20) Asp_{1040} (N_3, 3.42)	Glu_{878} (N_4, 3.87) Glu_{878} (H_4, 2.13)	Ile_{881} (C_{26}, 3.52) Ile_{882} (C_8, 3.36) Ile_{882} (C_{13}, 3.88) Ile_{882} (C_2, 3.34) Ile_{882} (C_3, 3.63) Ile_{882} (C_4, 3.69) Ile_{882} (C_5, 3.43) Ile_{882} (C_6, 3.16) Ile_{885} (C_{26}, 3.60) Val_{907} (C_{12}, 3.76) Val_{907} (C_{13}, 3.53) Val_{909} (C_8, 3.86) Val_{909} (C_{13}, 3.85) Val_{909} (C_9, 3.68) Val_{909} (C_{10}, 3.27) Val_{909} (C_{11}, 3.58) Val_{909} (C_{14}, 3.50) Cys_{1018} (C_{19}, 3.59) Leu_{1043} (C_{24}, 3.74)	
QDAU5	Cys_{1039} (O_1, 3.67)		Leu_{833} (C_{18}, 3.44) Leu_{833} (C_{19}, 3.45) Leu_{833} (C_{17}, 3.66) Leu_{833} (C_{20}, 3.72) Ala_{859} (C_{16}, 3.89) Ile_{881} (C_9, 3.56) Leu_{882} (C_{15}, 3.42) Leu_{882} (C_{14}, 3.48) Ile_{885} (C_8, 3.36) Val_{892} (C_3, 3.04) Val_{892} (C_4, 3.40) Val_{892} (C_2, 3.79) Val_{909} (C_3, 3.77) Leu_{1029} (C_1, 3.78) Leu_{1029} (C_{16}, 3.87) Cys_{1039} (C_3, 3.14) Cys_{1039} (C_4, 3.25)	Leu_{833} (F_2, 2.94)
6				Glu_{878} (C_{12}, 3.53) Ile_{1038} (C_{11}, 3.63) Asp_{1040} (C_{12}, 3.67)
12		Lys_{861} (O, 3.73)	Leu_{833} (C_7, 3.79) Leu_{833} (C_8, 3.26) Leu_{833} (C_9, 3.79) Ala_{859} (C_5, 3.78) Val_{892} (C_4, 3,89) Val_{909} (C_3, 3,34) Val_{909} (C_4, 3,74) Leu_{1029} (C_4, 3.74) Leu_{1029} (C_5, 3.42)	Asp_{1040} (F, 3.34)

Compound	Hydrogen bond	Polar Bond	Hydrophobic bond	Halogen bond
			Leu_{1029} (C_6, 3.72) Leu_{1029} (C_{10}, 3.64)	
27		Glu_{878} (O, 3.54)	Val_{841} (C_{11}, 3,30) Val_{841} (C_{10}, 3,54) Val_{892} (C_2, 3,66) Val_{892} (C_3, 3,24) Cys_{1039} (C_8, 3,57) Cys_{1039} (C_9, 3,83)	Asp_{1040} (F, 3.16)
29		Glu_{878} (O, 3.42)	Val_{841} (C_9, 3,74) Val_{841} (C_8, 3,22) Val_{892} (C_4, 3,04) Val_{892} (C_3, 3,34) Val_{909} (C_3, 3,75) Val_{892} (C_4, 3,37) Leu_{1029} (C_1, 3,29) Leu_{1029} (C_2, 3,26) Leu_{1029} (C_3, 3,72) Leu_{1029} (C_{10}, 3,81)	

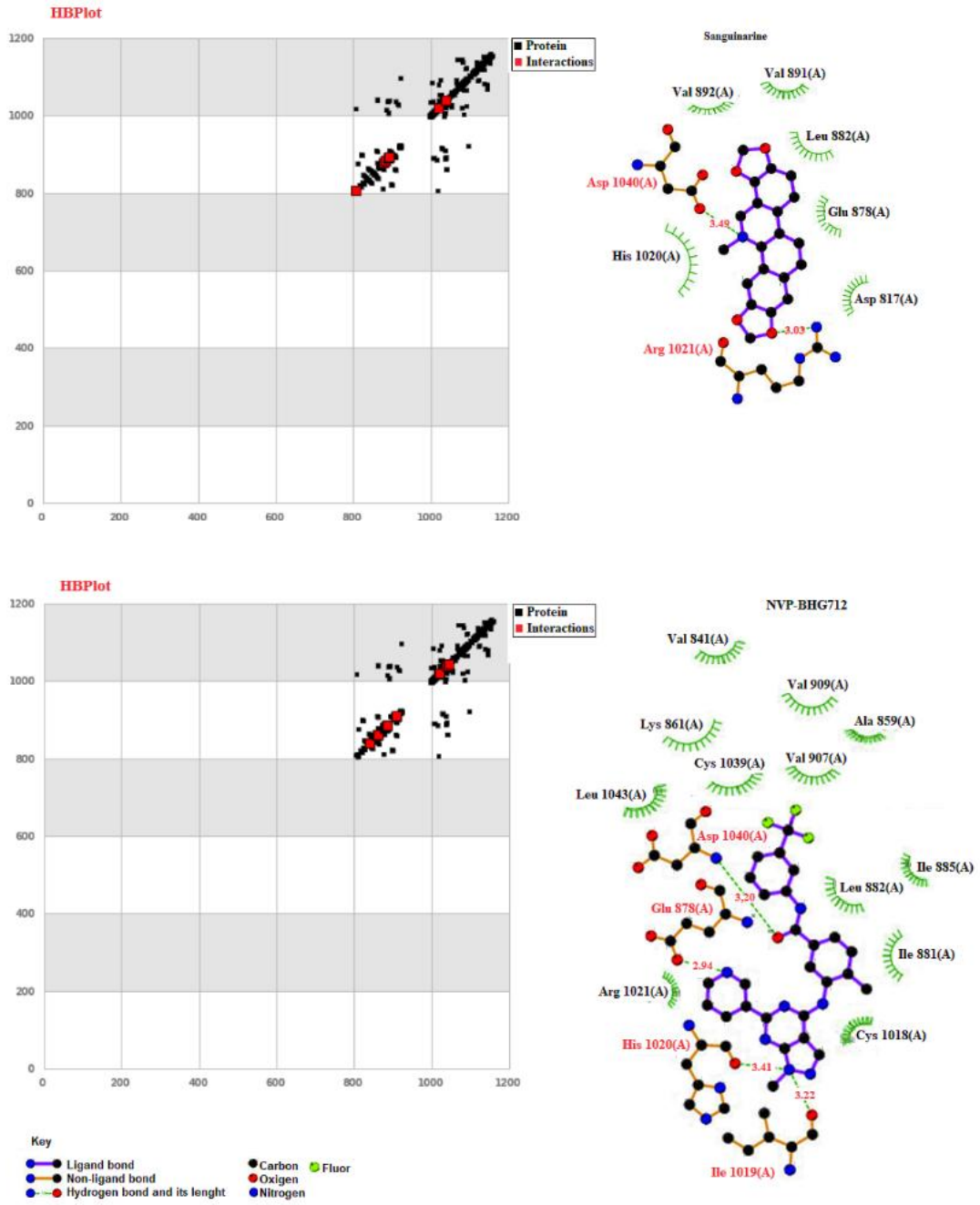

Figure 7. The scheme shows the coupling of sanguinarine and NVP-BHAG712 drugs with the 3HNG protein surface. Visualized with the DockingServer program.

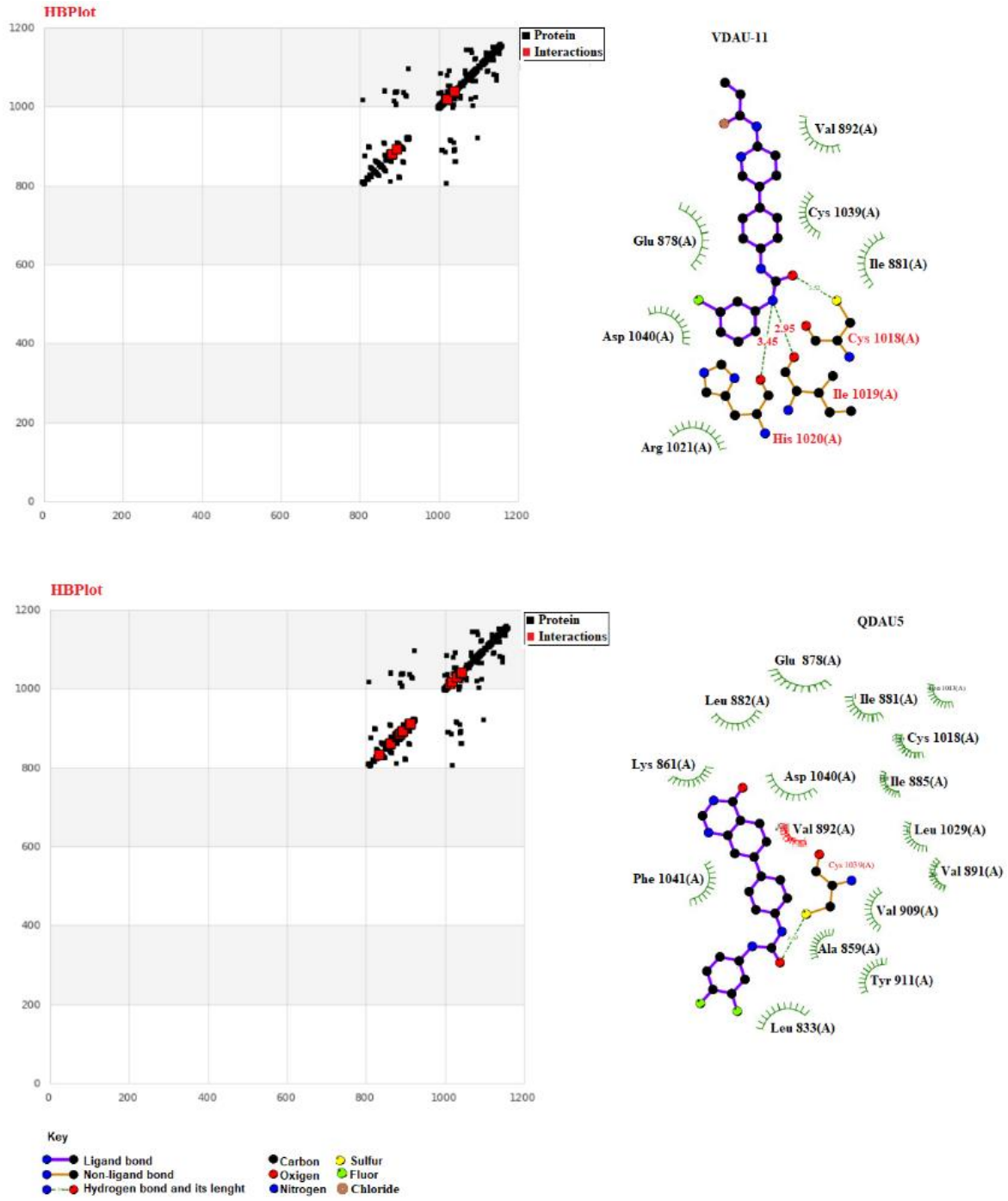

Figure 8. Coupling of VDAU-11 and QDAU5 drugs with 3HNG protein surface. Visualized with the DockingServer program.

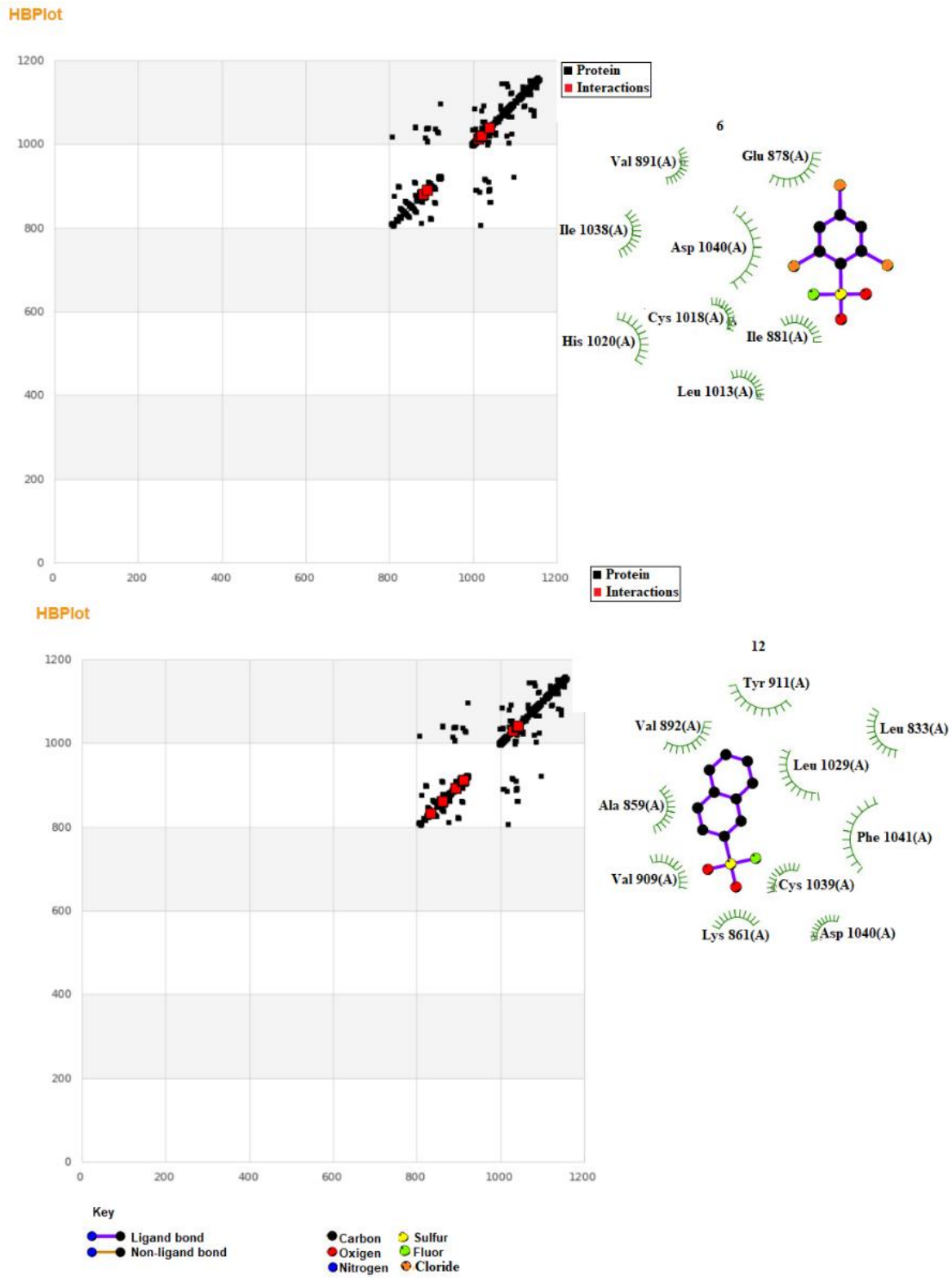

Figure 9. The scheme shows the interaction of fluoride derivatives 6 and 12 with the 3HNG protein surface. Visualized with the DockingServer program.

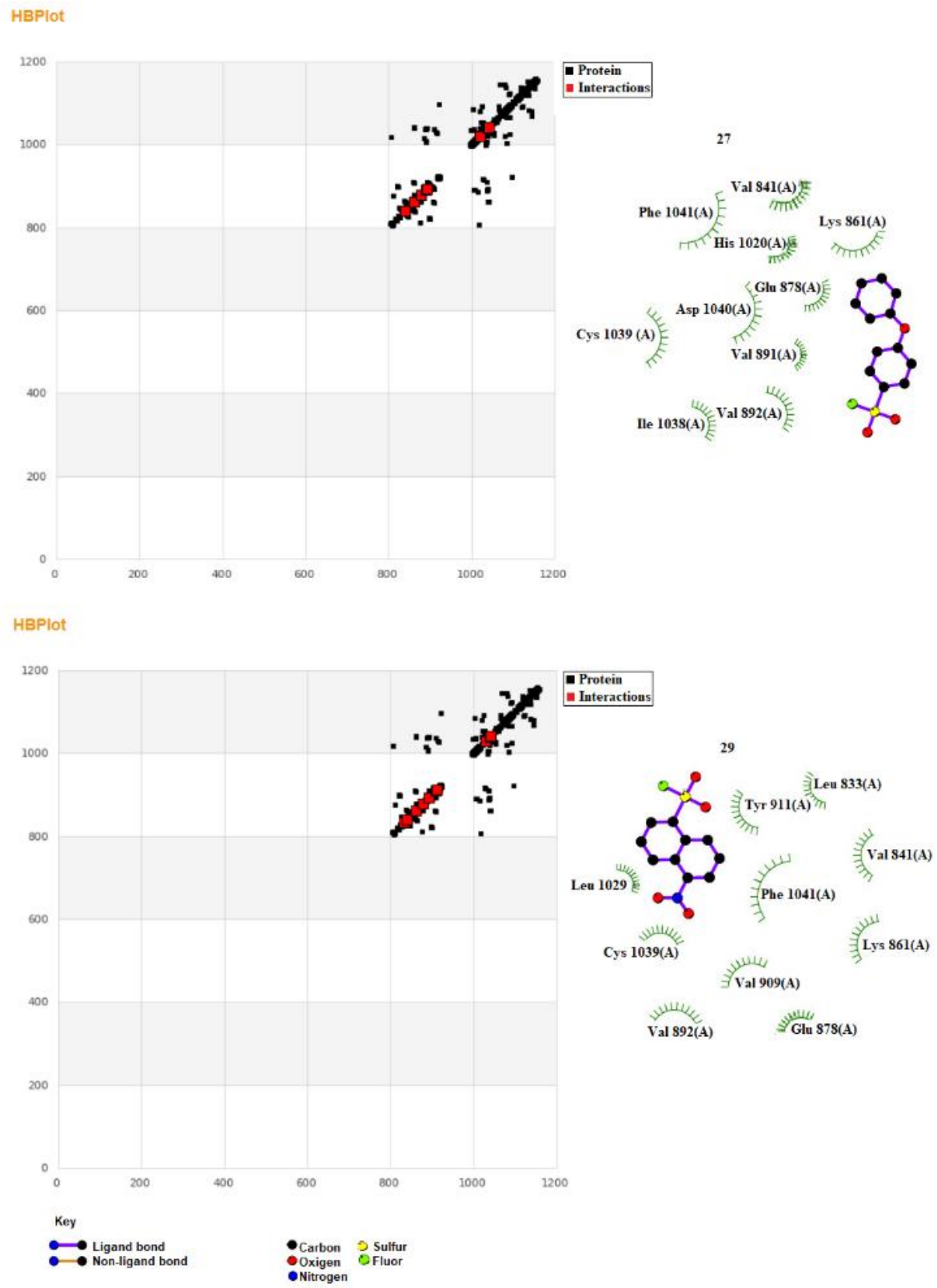

Figure 10. The coupling of fluoride derivatives 27 and 29 with the 3HNG protein surface. Visualized with the DockingServer program.

Table 9. Decomposed interaction energies in kcal/mol involved in the coupling of fluoride derivatives (6, 12, 27, and 29) with the 3HNG protein surface.

Compounds	Hydrogen bond	Polar Bond	Hydrophobic bond	Halogen bond
Sanguinarine	Asp_{104} (-1.171) Arg_{102} (-1.126)	Asp_{807} (-0.552)	His_{102} (-1.571) Leu_{882} (-0.743) Val_{891} (-0.312) Val_{892} (-0.243)	
QDAU5	Cys_{103} (-1.386)		Leu_{882} (-0.861)	

Compounds	Hydrogen bond	Polar Bond	Hydrophobic bond	Halogen bond
			Phe_{104} (-0.776) Val_{909} (-0.639) Tyr_{911} (-0.612) Ile_{881} (-0.466) Leu_{102} (-0.423) Ala_{859} (-0.407) Leu_{101} (-0.358) Ile_{885} (-0.145) Val_{892} (0.012)	
NVPBHG712	Asp_{104} (-1.825) His_{102} (-0.499) Ile_{101} (-0.280) Glu_{878} (-0.152)	Val_{909} (-1.024) Ile_{881} (-0.853) Leu_{882} (-0.718) Val_{907} (-0.603) Leu_{104} (-0.479) Ile_{885} (-0.287) Cys_{101} (-0.132)		
VDAU-11	His_{102} (-0.919) Cys_{101} (-0.367) Ile_{101} (0.068)	Arg_{102} (-0.833)	Ile_{881} (-0.781) Val_{892} (-0.682) Cys_{103} (-0.537)	Glu_{878} (-1.062) Asp_{104} (-0.729)
6				Asp_{104} (-1.2718) Glu_{878} (-0.6926) Ile_{8103} (-0.4264)
12		Lys_{861} (-0.3932)	Phe_{104} (-1.0691) Tyr_{911} (-0.7994) Leu_{102} (-0.7381) Val $_{892}$ (-0.5492) Leu_{833} (-0.5492) Val_{909} (-0.4368) Ala_{859} (-0.4273)	Asp_{104} (-0.225)
27		Glu_{878} (-0.3631)	Phe_{104} (-1.2605) Val $_{892}$ (-0.6451) Val $_{841}$ (-0.245)	Cys_{103} (-9273)
29		Glu_{878} (-0.1615)	Phe_{104} (-1.0673) Val_{909} (-0.5768) Val $_{892}$ (-0.5613) Val $_{841}$ (-0.5575) Leu_{102} (-0.2216)	

3.3. Pharmacokinetic parameters.

Table 10 shows some pharmacokinetic factors for fluoride derivatives (6, 10, 12, 27, and 29) and the controls (sanguinarine, VDAU-11, and QDAU5). The results showed that fluoride derivatives 10, 12, 27, and 29 may lower gastrointestinal absorption compared with the controls.

Table 10. Pharmacokinetic parameters for fluoride analogs (2, 6, 8, 31, and 32) and the controls.

Compound	*A*	*B*	*C*	*D*	*E*	*F*	*G*	*H*	*I*
Sanguinarine	High	Yes	Yes	Yes	Yes	No	No	No	2.88
VDAU1-11	High	No	No	Yes	Yes	Yes	No	Yes	3.45
QDAU5	High	No	No	Yes	No	No	Yes	No	3.73
6	High	Yes	No	Yes	Yes	Yes	No	Yes	3.66
10	Lower	No	No	No	Yes	Yes	No	No	2.29
12	Lower	No	No	No	No	No	No	No	2.71
27	Lower	No	No	No	Yes	Yes	No	No	3.22
29	Lower	No	No	Yes	Yes	Yes	No	Yes	2.14

A = GI absorption; *B* = BBB permeant; *C* = P-GP substrate; *D* = CYP1A2 inhibitor; *E* = CYP2C19 inhibitor; *F* = CYP2C9 inhibitor; *G* = CYP2D6 inhibitor; *H*= CYP3A4 inhibitor; *I* = Consensus Log $P_{O/W}$.

3.4. Toxicity analysis.

Table 11 shows the toxicity degree for fluoride analogs (6, 10, 12, 27, and 29) and the controls (sanguinarine, VDAU1-11, and QDAU5).

Table 11. The toxicity degree for fluoride derivatives (2, 6, 8, 31, and 32) and the controls was determined using Gussar software.

Compuesto	IP LD_{50} (mgkg)	IV LD_{50} (mgkg)	Oral LD_{50}(mgkg)	SC LD_{50}(mgkg)
Sanguinarine	469.90	52.48	964.40	465.50
VDAU-11	713.70	191.70	1790.00	2577.00
QDAU5	596.60	310.00	1428.00	1563.00
6	630.80	72.49	1374.00	473.00
10	481.80	70.75	1177.00	436.10
12	494.00	93.84	501.00	171.00
27	465.80	75.91	1670.00	471.90
29	145.10	67.14	1131.00	93.45

IP - Intraperitoneal route of administration; IV - Intravenous route of administration; Oral - Oral route of administration; SC - Subcutaneous route of administration.

3.5. Discussion.

3.5.1. First stage.

VEGFR-1 and EPHB4 are biomolecules linked to angiogenesis, tumor growth, and metastasis, making them viable targets for drug development to treat cancer cells. In this way, several drugs targeting VEGFR-1 and EPHB4, with biological activity, and their roles in tumorigenesis have been developed [30, 31]. For example, a study showed that an isoquinolone derivative can act as an EPHB4 inhibitor through fragment-based docking and molecular dynamics [38]. Other data indicate that the XL647 drug is a non-selective inhibitor of EphB4, EGFR (endothelial growth factor receptor), and HER2 (vascular endothelial growth factor receptor 2) used to treat cancer cells [39]. Furthermore, a report showed that the EphB4 kinase inhibitor NVP-BHG712 inhibits VEGF-induced angiogenesis in an in vitro model [30]. These data indicate that some VEGFR-1 and EPHB4 inhibitors have been used to treat cancer cells; however, it is necessary to develop additional compounds with biological activity against VEGFR-1 and EPHB4 to treat cancer. Based on this data, the aim of this study was to determine the interactions of 36 fluoride derivatives with VEGFR-1 and EPHB4 using different strategies. In the first stage, the coupling of the fluoride derivatives to EPHB4 was assessed using the 2VWX protein as a theoretical tool. Besides, sanguinarine, NVP-BHG712 (EphB4 inhibitor) [40], QDAU5 (triple inhibitor of VEGFR-2, Tie-2 (Tyrosine-protein kinase receptor) [41], and EphB4), and VDAU-11 (VEGFR-2, Tie-2, and EphB4 inhibitor) [31] were used as controls in the DockingServer program. The results showed differences in the number of amino acid residues involved in the coupling of fluoride derivatives with the 2VWX protein surface compared to the controls. Additionally, the inhibition constant (Ki) was lower for the fluoride derivatives 6 and 10 than for the compounds 1-5, 7-9, and 11-36. This phenomenon could be due to different types of bonds or different energy levels involved in the ligand-protein formation complex between fluoride derivatives 6 and 10 with the 2VWX protein surface. Other results displayed different binding energy levels for fluoride derivatives 6 and 10 compared with the controls. In addition, other data indicate that the fluoride derivatives 6 and 10 may interact with the amino acid residues Glu669 and Thr693 via halogen bonds. Additionally, other data indicate that fluoride derivative 6 interacts with Glu_{664} through a hydrogen bond. Finally, compound 6 may interact with Ser_{757} via a polar bond.

3.5.2. Second stage.

The ligand-protein complex formation between fluoride derivatives and the 3HNG protein achieved the second stage. The results showed differences in the number of amino acids

involved in the coupling of fluoride derivatives with the 3HNG protein surface. Besides, the binding free energy levels for fluoride derivatives were different compared with the controls. Other data indicate that the Ki for the compounds 6, 12, 27, and 29 was lower compared with fluoride derivatives 1-5, 7-11, 13-26, 28, and 30-36. Besides, the Ki values for the fluoride derivatives 1-36 were higher than those of the controls. Other results show that fluoride derivative 6 may interact with the amino acid residue Asp_{1040} through a halogen bond. In addition, some data suggest that fluoride derivatives 27 and 29 may interact with Glu_{878} via a polar bond.

3.5.3. Pharmacokinetic analysis.

In the literature, several methods are available to determine pharmacokinetic parameters associated with the biological activity of various drugs, such as GastroPlus@ [42], PKMP [43], NONMEM [44], PBPK [45], SwissADME [36], and others. In this study, pharmacokinetic data for fluoride derivatives (6, 10, 12, 27, and 29) were determined using the SwissADME software. The results indicated that the fluoride derivative 6 may have higher gastrointestinal absorption compared with the compounds 10, 12, 27, and 29. Other results indicate that compounds 6 and 29 may act as CYP1A2 and CYP3A4 inhibitors. Furthermore, the fluoride derivatives 6, 10, 27, and 29 can interact with CYP2C19 and CYP2C9.

On the other hand, other data showed that the lipophilicity of the fluoride analog 6 was higher than that of compounds 10, 12, 27, and 29. Furthermore, compound QDAU5 shows a high degree of lipophilicity compared to sanguinarine, VDAU-11, and the fluoride derivatives (6, 10, 12, 27, and 29). Therefore, it would be expected that QDAU5 would be able to cross the blood-brain barrier (BBB) more easily than sanguinarine, VDAU-11, and compounds 6, 10, 12, 27, and 29. This phenomenon may be because the SwissADME program considers other factors, such as the chemical structure of the compounds and the percentage of the drug that could reach the target cell or receptor.

3.5.4. Toxicology degree.

In the literature, there are reports on the toxicity of fluorinated compounds [46, 47]; therefore, in this study, the toxicity was assessed using a theoretical model. It is important to note that several methods, such as ToxCast [48], ToxII [49], Genetox [50], Osiris [51], and Gussar [52], can predict the toxicity of different drugs. In this study, the toxicity of fluoride derivatives (6, 10, 12, 27, and 29) was determined using Gussar software and compared with the controls (sanguinarine, VDAU-11, and QDAU5). The results showed that the fluorinated derivative 12 requires a higher dose to produce toxicity via the intraperitoneal route than compounds 6, 10, 27, 29, and the sanguinarine drug. Other data indicate that compound 29 requires lower doses via the intraperitoneal route to produce toxicity than compounds 6, 10, 12, and the controls. Finally, compound 27 requires higher oral doses than compounds 6, 10, 12, 29, sanguinarine, and QDAU5. All these data suggest that the degree of toxicity of each compound could depend on the chemical characteristics of each fluorinated derivative; however, it is important to mention that for a chemical substance to produce toxicity, it involves several processes, including the route of administration and some metabolic processes, before reaching its site of action and reacting with a biomolecule. Therefore, methods for predicting the degree of toxicity from chemical structure can make a valuable contribution to the early detection of potentially toxic chemicals.

4. Conclusions

In conclusion, all these data suggest the following: 1) Fluoride derivatives 6 and 10 could have a higher affinity for 2VWZ compared to compounds 1-5, 7-9 and 11-36; 2) fluorinated analogs 6, 12, 27, and 29 could have a higher affinity for 3HNG compared to compounds 1-5, 7-11, 13-26, 28, and 30-36. All these data suggest that fluorinated derivatives 6, 10, 12, 27, and 29 may act as VEGFR-1 and EphB4 inhibitors. Therefore, these fluoride derivatives may be good candidates to evaluate their biological activity in some cancer cell lines.

Author Contributions

Conceptualization – R.-N.M., A.-R.M.; Data curation – R.-N.M.; Formal analysis – R.-N.M., A.-R.M., M.-G.M.A., R.-H.A., R.-D.M.P.; Funding acquisition – R.-N.M., A.-R.M., B.-Z.E., M.-G.M.A., R.-H.A.; Investigation – R.-N.M., A.-R.M., B.-Z.E., M.-G.M.A., R.-H.A., R.-D.M.P.; Methodology – R.-N.M., A.-R.M., B.-Z.E.; Visualization – R.-N.M., A.-R.M., B.-Z.E., M.-G.M.A., R.-H.A., R.-D.M.P.; Writing – original draft preparation – R.-N.M., A.-R.M.; Writing – review & editing – R.-N.M., A.-R.M., B.-Z.E., M.-G.M.A., R.-H.A. All authors have read and agreed to the published version of the manuscript.

Institutional Review Board Statement

Not applicable.

Informed Consent Statement

Not applicable.

Data Availability Statement

The data that support the findings of this study are available from the corresponding author upon reasonable request.

Funding

The authors received no specific funding for this work.

Acknowledgments

None.

Conflicts of Interest

Authors declare no conflicts of interest.

References

1. Sobczyńska-Rak, A.; Żylińska, B.; Nowicka, B.; Rak, E.; Rzepka, T. Role and Mechanisms of Angiogenesis in Tumours. *Biology* **2025**, *14*, 756, https://doi.org/10.3390/biology14070756.
2. Jensen, L.; Guo, Z.; Sun, X.; Jing, X.; Yang, Y.; Cao, Y. Angiogenesis, signaling pathways, and animal models. *Chin. Med. J.* **2025**, *138*, 1153-1162, https://doi.org/10.1097/cm9.0000000000003561.

3. Yang, S.; Fang, Y.; Ma, Y.; Wang, F.; Wang, Y.; Jia, J.; Yang, Y.; Sun, W.; Zhou, Q.; Li, Z. Angiogenesis and targeted therapy in the tumour microenvironment: From basic to clinical practice. *Clin. Transl. Med.* **2025**, *15*, e70313, https://doi.org/10.1002/ctm2.70313.
4. Trun, W.; Fernández-Montalván, A.; Cao, Y.-J.; Haendler, B.; Zopf, D. Inhibition of EphB4 Receptor Signaling by Ephrin-B2-Competitive and Non-Competitive DARPins Prevents Angiogenesis. *Biochemistry* **2025**, *64*, 620-633, https://doi.org/10.1021/acs.biochem.4c00431.
5. Lin, Y.; Zhan, M.; Chen, X.; Xiao, X. Biological function of EPHB4 in the aging process of vascular endothelial cells: mtDNA molecular mechanism and MAPK/PGC-1/TFAM signaling pathway. *Int. J. Biol. Macromol.* **2025**, *293*, 138536, https://doi.org/10.1016/j.ijbiomac.2024.138536.
6. Tu, M.; Xu, H.; Miao, Z.; Wang, Y.; Feng, X.; Xie, L.; Wang, F. Interleukin 29 is a novel antiangiogenic factor in angiogenesis. *Cytokine* **2025**, *186*, 156850, https://doi.org/10.1016/j.cyto.2024.156850.
7. Peluzzo, A.M.; Autieri, M.V. Challenging the Paradigm: Anti-Inflammatory Interleukins and Angiogenesis. *Cells* **2022**, *11*, 587, https://doi.org/10.3390/cells11030587.
8. Kaur, G.; Roy, B. Decoding Tumor Angiogenesis for Therapeutic Advancements: Mechanistic Insights. *Biomedicines* **2024**, *12*, 827, https://doi.org/10.3390/biomedicines12040827.
9. Cazzato, G.; Ingravallo, G.; Ribatti, D. Angiogenesis Still Plays a Crucial Role in Human Melanoma Progression. *Cancers* **2024**, *16*, 1794, https://doi.org/10.3390/cancers16101794.
10. Wang, M.; Xu, C.; Wang, D.; Lu, J.; Wang, A.; Zhou, Q. Analysis of current trends in angiogenesis research for wound healing: A bibliometric study from 2013 to 2023. *Heliyon* **2024**, *10*, e32311, https://doi.org/10.1016/j.heliyon.2024.e32311.
11. Xu, B.; Wu, Z.; Lin, Y.; Liu, Y.; Liu, L.; Zhang, Y. Association of plasma VEGF with futile recanalization and intracranial angiogenesis in ischemic stroke post-endovascular treatment. *J. Clin. Neurosci.* **2024**, *129*, 110831, https://doi.org/10.1016/j.jocn.2024.110831.
12. Guo, Z.; Jing, X.; Sun, X.; Sun, S.; Yang, Y.; Cao, Y. Tumor angiogenesis and anti-angiogenic therapy. *Chinese Medical Journal* **2024**, *137*, 2043-2051, https://doi.org/10.1097/cm9.0000000000003231.
13. Ngaha, T.Y.; Zhilenkova, A.V.; Essogmo, F.E.; Uchendu, I.K.; Abah, M.O.; Fossa, L.T.; Sangadzhieva, Z.D.; D. Sanikovich, V.; S. Rusanov, A.; N. Pirogova, Y.; Boroda, A.; Rozhkov, A.; Kemfang Ngowa, J.D.; N. Bagmet, L.; I. Sekacheva, M. Angiogenesis in Lung Cancer: Understanding the Roles of Growth Factors. *Cancers* **2023**, *15*, 4648 https://doi.org/10.3390/cancers15184648.
14. Lv, J.; Xia, Q.; Wang, J.; Shen, Q.; Zhang, J.; Zhou, X. EphB4 promotes the proliferation, invasion, and angiogenesis of human colorectal cancer. *Exp. Mol. Pathol.* **2016**, *100*, 402-408, https://doi.org/10.1016/j.yexmp.2016.03.011.
15. Corbo, S.; Nguyen, D.; Bhatia, S.; Darragh, L.B.; Abdelazeem, K.N.M.; Court, B.V.; Olimpo, N.A.; Gadwa, J.; Yu, J.; Hodgson, C.; Samedi, V.; Garcia, E.S.; Siu, L.; Saviola, A.; Heasley, L.E.; Knitz, M.W.; Pasquale, E.B.; Karam, S.D. The pro-tumoral and anti-tumoral roles of EphA4 on T regulatory cells and tumor associated macrophages during HNSCC tumor progression. *bioRxiv* **2024**, 2024.2008.2013.607778, https://doi.org/10.1101/2024.08.13.607778.
16. Al-Jamaei, A.A.H.; Subramanyam, R.V.; Helder, M.N.; Forouzanfar, T.; van der Meij, E.H.; Al-Jamei, S.; de Visscher, J.G.A.M. A narrative review of the role of Eph receptors in head and neck squamous cell carcinoma. *Oral Dis.* **2024**, *30*, 833-845, https://doi.org/10.1111/odi.14625.
17. Bhatia, S.; Nguyen, D.; Darragh, L.B.; Van Court, B.; Sharma, J.; Knitz, M.W.; Piper, M.; Bukkapatnam, S.; Gadwa, J.; Bickett, T.E.; Bhuvane, S.; Corbo, S.; Wu, B.; Lee, Y.; Fujita, M.; Joshi, M.; Heasley, L.E.; Ferris, R.L.; Rodriguez, O.; Albanese, C.; Kapoor, M.; Pasquale, E.B.; Karam, S.D. EphB4 and ephrinB2 act in opposition in the head and neck tumor microenvironment. *Nat. Commun.* **2022**, *13*, 3535, https://doi.org/10.1038/s41467-022-31124-7.
18. Xu, C.; Gu, L.; Kuerbanjiang, M.; Jiang, C.; Hu, L.; Liu, Y.; Xue, H.; Li, J.; Zhang, Z.; Xu, Q. Adaptive activation of EFNB2/EPHB4 axis promotes post-metastatic growth of colorectal cancer liver metastases by LDLR-mediated cholesterol uptake. *Oncogene* **2023**, *42*, 99-112, https://doi.org/10.1038/s41388-022-02519-z.
19. Li, G.X.; Ma, B.; Zhang, S.; Liu, R.; Siddiqi, I.N.; Sali, A.; El-Khoueiry, A.; Gross, M.; Salhia, B.; Sadeghi, S.; Gill, P.S. EphB4-ephrin-B2 are targets in castration resistant prostate cancer. *Br. J. Cancer* **2025**, *132*, 679-689, https://doi.org/10.1038/s41416-025-02942-5.
20. Groppa, E.; Brkic, S.; Uccelli, A.; Wirth, G.; Korpisalo-Pirinen, P.; Filippova, M.; Dasen, B.; Sacchi, V.; Muraro, M.G.; Trani, M.; Reginato, S.; Gianni-Barrera, R.; Ylä-Herttuala, S.; Banfi, A. EphrinB2/EphB4

signaling regulates non-sprouting angiogenesis by VEGF. *EMBO Rep.* **2018**, *19*, EMBR201745054, https://doi.org/10.15252/embr.201745054.

21. Masumura, T.; Yamamoto, K.; Shimizu, N.; Obi, S.; Ando, J. Shear Stress Increases Expression of the Arterial Endothelial Marker EphrinB2 in Murine ES Cells via the VEGF-Notch Signaling Pathways. *Arterioscler. Thromb. Vasc. Biol.* **2009**, *29*, 2125-2131, https://doi.org/10.1161/ATVBAHA.109.193185.
22. Thomas, J.-L.; Baker, K.; Han, J.; Calvo, C.; Nurmi, H.; Eichmann, A.C.; Alitalo, K. Interactions between VEGFR and Notch signaling pathways in endothelial and neural cells. *Cell. Mol. Life Sci.* **2013**, *70*, 1779-1792, https://doi.org/10.1007/s00018-013-1312-6.
23. Liu, X.; Zhang, J.; Yi, T.; Li, H.; Tang, X.; Liu, D.; Wu, D.; Li, Y. Decoding tumor angiogenesis: pathways, mechanisms, and future directions in anti-cancer strategies. *Biomark. Res.* **2025**, *13*, 62, https://doi.org/10.1186/s40364-025-00779-x.
24. Figueroa-Valverde, L.; Rosas-Nexticapa, M.; Alvarez-Ramirez, M.; Mateu-Armad, M.V.; Cauich-Carrillo, R. Theoretical interaction of muscarinic receptor antagonist with vascular endothelial growth factor receptors (VEGF-R1, R2 and R3) as a therapeutic alternative to treat cancer. *Braz. J. Sci.* **2025**, *4*, 1-14, https://doi.org/10.14295/bjs.v4i5.734.
25. Figueroa-Valverde, L.; Díaz-Cedillo, F.; Rosas-Nexticapa, M.; Alvarez-Ramirez, M.; Mateu-Armad, M.V.; López-Ramos, M.; López-Gutierrez, T. Interaction of Some Amino-Nitrile Derivatives with Vascular Endothelial Growth Factor Receptor 1 (VEGFR1) Using a Theoretical Model. *Drug Res.* **2023**, *73*, 355-364, https://doi.org/10.1055/a-2062-3571.
26. Konrad, D.; Marcin, O.; Beniamin Oskar, G.; Nikola, Z.; Barbara, T.; Tomasz, H.; Ewa, L.; Krzysztof, J.; Ryszard, B.; Robert, K.; Dariusz, B. Changes in the Expression Profile of VEGF-A, VEGF-B, VEGFR-1, VEGFR-2 in Different Grades of Endometrial Cancer. *Curr. Pharm. Biotechnol.* **2019**, *20*, 955-963, https://doi.org/10.2174/1389201020666190717092448.
27. Hu, Y.; Fang, Q. Analysis of research hotspots on the detection of vascular endothelial growth factor C and its receptor vascular endothelial growth factor receptor-3 in cervical squamous cell carcinoma. *Discov. Oncol.* **2025**, *16*, 2315, https://doi.org/10.1007/s12672-025-04034-5.
28. Mehnert, J.M.; McCarthy, M.M.; Aziz, S.A.; Sznol, M.; Flaherty, K.T.; Camp, R.L.; Rimm, D.L.; Kluger, H.M. VEGF, VEGFR1, and VEGFR2 expression in melanoma. *J. Clin. Oncol.* **2007**, *25*, 8520-8520, https://doi.org/10.1200/jco.2007.25.18_suppl.8520.
29. Klasa-Mazurkiewicz, D.; Jarząb, M.; Milczek, T.; Lipińska, B.; Emerich, J. Clinical significance of VEGFR-2 and VEGFR-3 expression in ovarian cancer patients. *Pol. J. Pathol.* **2011**, *62*, 31-40.
30. Martiny-Baron, G.; Holzer, P.; Billy, E.; Schnell, C.; Brueggen, J.; Ferretti, M.; Schmiedeberg, N.; Wood, J.M.; Furet, P.; Imbach, P. The small molecule specific EphB4 kinase inhibitor NVP-BHG712 inhibits VEGF driven angiogenesis. *Angiogenesis* **2010**, *13*, 259-267, https://doi.org/10.1007/s10456-010-9183-z.
31. Li, C.; Shan, Y.; Sun, Y.; Si, R.; Liang, L.; Pan, X.; Wang, B.; Zhang, J. Discovery of novel anti-angiogenesis agents. Part 7: Multitarget inhibitors of VEGFR-2, TIE-2 and EphB4. *Eur. J. Med. Chem.* **2017**, *141*, 506-518, https://doi.org/10.1016/j.ejmech.2017.10.030.
32. Bardelle, C.; Coleman, T.; Cross, D.; Davenport, S.; Kettle, J.G.; Ko, E.J.; Leach, A.G.; Mortlock, A.; Read, J.; Roberts, N.J.; Robins, P.; Williams, E.J. Inhibitors of the tyrosine kinase EphB4. Part 2: Structure-based discovery and optimisation of 3,5-*bis* substituted anilinopyrimidines. *Bioorg. Med. Chem. Lett.* **2008**, *18*, 5717-5721, https://doi.org/10.1016/j.bmcl.2008.09.087.
33. Bikadi, Z.; Hazai, E. Application of the PM6 semi-empirical method to modeling proteins enhances docking accuracy of AutoDock. *Journal of cheminformatics* **2009**, *1*(1), 15. http://www.jcheminf.com/content/1/1/15
34. Morris, G.; Goodsell, D.; Halliday, R.; Huey, R.; Hart, W.; Belew, R.; Olson, A. Automated docking using a Lamarckian genetic algorithm and an empirical binding free energy function. *Journal of computational chemistry* **1998**, *19*(14), 1639-1662.
35. Solis, F.; Wets, R. Minimization by random search techniques. *Mathematics of operations research* **1981**, *6*(1), 19-30.
36. Bakchi, B.; Krishna, A.D.; Sreecharan, E.; Ganesh, V.B.J.; Niharika, M.; Maharshi, S.; Puttagunta, S.B.; Sigalapalli, D.K.; Bhandare, R.R.; Shaik, A.B. An overview on applications of SwissADME web tool in the design and development of anticancer, antitubercular and antimicrobial agents: A medicinal chemist's perspective. *J. Mol. Struct.* **2022**, *1259*, 132712, https://doi.org/10.1016/j.molstruc.2022.132712.
37. Khrapova, M.V.; Khrapov, S.E.; Chechushkov, A.V.; Kozhin, P.M.; Romakh, L.P.; Serykh, A.E.; Kholshin, S.V.; Kandalintseva, N.V.; Menshchikova, E.B. The Toxicity of a New Monophenolic Synthetic

Inducer of Keap1/Nrf2/ARE Redox-Sensitive Signaling System In Vitro and In Vivo. *Cell Tiss. Biol.* **2023**, *17*, 299-305, https://doi.org/10.1134/S1990519X23030069.
38. Zhao, H.; Dong, J.; Lafleur, K.; Nevado, C.; Caflisch, A. Discovery of a Novel Chemotype of Tyrosine Kinase Inhibitors by Fragment-Based Docking and Molecular Dynamics. *ACS Med. Chem. Lett.* **2012**, *3*, 834-838, https://doi.org/10.1021/ml3001984.
39. Pietanza, M.C.; Gadgeel, S.M.; Dowlati, A.; Lynch, T.J.; Salgia, R.; Rowland, K.M.; Wertheim, M.S.; Price, K.A.; Riely, G.J.; Azzoli, C.G.; Miller, V.A.; Krug, L.M.; Kris, M.G.; Beumer, J.H.; Tonda, M.; Mitchell, B.; Rizvi, N.A. Phase II Study of the Multitargeted Tyrosine Kinase Inhibitor XL647 in Patients with Non–Small-Cell Lung Cancer. *J. Thorac. Oncol.* **2012**, *7*, 856-865, https://doi.org/10.1097/JTO.0b013e31824c943f.
40. Martiny-Baron, G.; Holzer, P.; Billy, E.; Schnell, C.; Brueggen, J.; Ferretti, M.; Schmiedeberg, N.; Wood, J.M.; Furet, P.; Imbach, P. The small molecule specific EphB4 kinase inhibitor NVP-BHG712 inhibits VEGF driven angiogenesis. *Angiogenesis* **2010**, *13*, 259-267, https://doi.org/10.1007/s10456-010-9183-z.
41. Zhang, L.; Shan, Y.; Ji, X.; Zhu, M.; Li, C.; Sun, Y.; Si, R.; Pan, X.; Wang, J.; Ma, W. Discovery and evaluation of triple inhibitors of VEGFR2 TIE2 and EphB4 as antiangiogenic and anticancer agents. *Oncotarget* **2017**, *8*, 104745–104760, https://doi.org/10.18632/oncotarget.20065.
42. Almajidi, Y.Q.; Faisal, R.R.; Yaseen, A. GastroPlus® as simulating/conducting software for modeling physiologically-based pharmacokinetics & physiologically based biopharmaceutics. *Maaen J. Med. Sci.* **2025**, *4*, 10, https://doi.org/10.55810/2789-9136.1078.
43. Gutierrez, L.; Hernández, M.; Del Villar, J.L.; Sánchez, Z.; Sumano, H. Pharmacokinetic evaluation of a long-acting, tasteless oral formulation of enrofloxacin in dogs. *Open Vet. J.* **2025**, *15*, 5009-5017, https://doi.org/10.5455/ovj.2025.v15.i10.19.
44. Yu, B.; Mei, K.; Zhan, D.; Tang, Q.; Cai, H.; Zhang, R. Establishment of a Vancomycin Population Pharmacokinetic Model for Pediatric Patients Based on the Non-Linear Mixed-Effects Model. *Drugs R D* **2025**, *25*, 309-320, https://doi.org/10.1007/s40268-025-00523-8.
45. Li, Y.; Sun, H.; Zhang, Z. The Evolution and Future Directions of PBPK Modeling in FDA Regulatory Review. *Pharmaceutics* **2025**, *17*, 1413, https://doi.org/10.3390/pharmaceutics17111413.
46. Johnston, N.R.; Strobel, S.A. Principles of fluoride toxicity and the cellular response: a review. *Arch. Toxicol.* **2020**, *94*, 1051-1069, https://doi.org/10.1007/s00204-020-02687-5.
47. Murphy, C.D.; Sandford, G. Recent advances in fluorination techniques and their anticipated impact on drug metabolism and toxicity. *Expert Opin. Drug Metab. Toxicol.* **2015**, *11*, 589-599, https://doi.org/10.1517/17425255.2015.1020295.
48. Kim, D.; Ahn, S.; Choi, J. Identification of developmental and reproductive toxicity of biocides in consumer products using ToxCast bioassays data and machine learning models. *Environ. Int.* **2025**, *202*, 109621, https://doi.org/10.1016/j.envint.2025.109621.
49. Ortiz-Andrade, R.; Araujo-León, J.A.; Sánchez-Recillas, A.; Navarrete-Vazquez, G.; González-Sánchez, A.A.; Hidalgo-Figueroa, S.; Alonso-Castro, Á.J.; Aranda-González, I.; Hernández-Núñez, E.; Coral-Martínez, T.I.; Sánchez-Salgado, J.C.; Yáñez-Pérez, V.; Lucio-Garcia, M.A. Toxicological Screening of Four Bioactive Citroflavonoids: In Vitro, In Vivo, and In Silico Approaches. *Molecules* **2020**, *25*, 5959, https://doi.org/10.3390/molecules25245959.
50. Mendes da Silva, L.; Andrade–Vieira, L.F. Ecotoxicological bioassays with terrestrial plants: a holistic view of standards, guidelines, and protocols. *J. Toxicol. Environ. Health B Crit. Rev.* **2025**, *28*, 183-221, https://doi.org/10.1080/10937404.2024.2440876.
51. Srivastava, R. Theoretical Studies on the Molecular Properties, Toxicity, and Biological Efficacy of 21 New Chemical Entities. *ACS Omega* **2021**, *6*, 24891-24901, https://doi.org/10.1021/acsomega.1c03736.
52. Askerova, U. Prediction of acute toxicity for (Z)-3-(2-phenylhydrazinylidene)benzofuran-2(3H)-one and its derivatives for rats using Gusar program. *New Materials, Compounds and Applications* **2023**, *7*, 50-56.

Publisher's Note & Disclaimer

The statements, opinions, and data presented in this publication are solely those of the individual author(s) and contributor(s) and do not necessarily reflect the views of the publisher and/or the editor(s). The publisher and/or the editor(s) disclaim any responsibility for the accuracy, completeness, or reliability of the content. Neither the publisher nor the editor(s) assume any legal liability for any errors, omissions, or consequences arising from the use of the information presented in this publication. Furthermore, the publisher and/or the editor(s) disclaim any

liability for any injury, damage, or loss to persons or property that may result from the use of any ideas, methods, instructions, or products mentioned in the content. Readers are encouraged to independently verify any information before relying on it, and the publisher assumes no responsibility for any consequences arising from the use of materials contained in this publication.